Ex libris
UNIVERSITATIS
ALBERTENSIS

The Bruce Peel
Special Collections
Library

Digitized by the Internet Archive
in 2025 with funding from
University of Alberta Library

https://archive.org/details/0162014920175

University of Alberta

Library Release Form

Name of Author: Jennifer Lynn Brown

Title of Thesis: Modal Decomposition of Convection-Reaction-Diffusion Systems

Degree: Master of Science

Year this Degree Granted: 2001

Permission is hereby granted to the University of Alberta Library to reproduce single copies of this thesis and to lend or sell such copies for private, scholarly or scientific research purposes only.

The author reserves all other publication and other rights in association with the copyright in the thesis, and except as hereinbefore provided, neither the thesis nor any substantial portion thereof may be printed or otherwise reproduced in any material form whatever without the author's prior written permission.

"In mathematics you don't understand things. You just get used to them."
von Neumann, Johann (1903 - 1957)

University of Alberta

Modal Decomposition of Convection-Reaction-Diffusion Systems

by

Jennifer Lynn Brown ©

A thesis submitted to the Faculty of Graduate Studies and Research in partial fulfillment of the requirements for the degree of **Master of Science**.

in

Process Control

Department of Department of Chemical and Materials Engineering

Edmonton, Alberta
Fall 2001

University of Alberta

Faculty of Graduate Studies and Research

The undersigned certify that they have read, and recommend to the Faculty of Graduate Studies and Research for acceptance, a thesis entitled **Modal Decomposition of Convection-Reaction-Diffusion Systems** submitted by Jennifer Lynn Brown in partial fulfillment of the requirements for the degree of **Master of Science** in *Process Control.*

To my Dad...

for all the times you helped with the little stuff,
but most of all for all the love and support.

Abstract

Many industrial processes have states and outputs that vary both spatially and temporally (e.g., heat treating / exchange and sheet forming processes, tubular (bio)reactors). Such processes are termed distributed parameter systems (DPS) and their dynamics are described by partial differential equations (PDEs). Current control approaches for DPS are based on a discretization of the PDE model, which yields a large number of ordinary differential equations in time. An alternative approach is modal decomposition analysis. This technique uses eigenfunction expansion to reduce the DPS model to a set of ODEs that are fully decoupled in the modal space. Modal decomposition is applied to a linear convection-diffusion-reaction system and a model predictive controller is designed in the modal space. Also modal decomposition is applied to an industrial problem (pulp bleaching reactor) modeled by a set of nonlinear PDEs; the resulting eigenfunctions of the spatial operator are Modified Bessel functions of complex order.

Acknowledgements

I would like to express gratitute to my two supervisors Dr. Fraser Forbes and Dr. Michel Perrier. Dr. Forbes provided guidance and kept me focused despite the fact that we were more often than not separated by 4000 km, and Dr. Perrier made me feel very welcome at Ecole Polytechnique and provided great help especially with debugging nasty programs. I would also like to thank all the members of the University of Alberta CPC group as well as the URCPC for their friendship and support as well as their technical feedback over the course of my project. The financial support of NSERC as well as the department of Chemical and Materials Engineering at the University of Alberta is greatfully acknowleged. To my parents, other family, and friends (especially Alex), I owe a great amount of thanks for putting up with my moods, frustrations, tantrums, and many tears over the past two years. Without you I wouldn't have been able to get through this. And last, but certainly not least, un gros merci à Denis...Sans toi, tout cela n'aurait pas été possible. Sans ta patience (même si on s'est faché quelques fois parce ce que je suis bornée!), tes encouragements, je n'aurais jamais eu le courage de continuer et de finir. Quand je t'ai rencontré pour la première fois, je n'aurais jamais pensé que ce coureur de marathon deviendrait un de mes meilleurs amis... Merci

Contents

1 **Introduction** 1

1.1 Distributed Parameter Systems 1

1.2 Control of Distributed Parameter Systems 2

1.3 Thesis Scope and Objectives 3

2 **Modelling and System Background** 5

2.1 PDE Classification 6

2.2 Hyperbolic PDEs 7

2.3 Elliptic PDEs 7

2.4 Parabolic PDEs 8

2.5 Model Requirements for Problem Formulation 8

2.6 General Solution Methods 9

2.6.1 Finite Difference Approximations 9

2.6.2 Numerical Techniques Using Weighted Residual Methods (WRM) . 10

2.7 Modal Decomposition 12

2.7.1 Parabolic Example: Heat Equation 13

2.8 Summary 16

3 **Modal Decomposition for Parabolic Diffusion-Reaction Systems** 18

3.1 Convection-Diffusion-Reaction Model 18

3.1.1 Model with linear reaction kinetics 19

3.1.2 Converting inhomogeneous boundary conditions 20

3.1.3 Modal decomposition 20

3.1.4 Simulation Examples 21

3.2 Application Example - MPC in the modal space 23

3.2.1 Simulations 26

3.2.2 Discussion 28

4 **Modal Decomposition of a Bleaching Reactor Model** 30

4.1 Chemical Bleaching Process 31

4.2 Bleaching Reactor Model 32

4.2.1 Nonlinear Model and Linear Tangent Model 32
4.2.2 Numerical Solution of Steady State Profiles 34
4.3 Modal Decomposition 38
4.3.1 Triangularized System 38
4.3.2 Decomposition of First PDE 39
4.3.3 Simulation 40
4.3.4 Decomposition using Eigenfunction Expansion - Second PDE: 41
4.3.5 Solution of Spatial ODE 43
4.3.6 Application of Boundary conditions: determination of eigenvalues . 45
4.4 Simulation Results 48
4.4.1 Discussion 51

5 Summary and Conclusions **53**

Bibliography **56**

A Nomenclature **59**

B PDE Solution Methods **62**
B.1 Method of Characteristics 62
B.2 Finite Differences 63

C Model Predictive Control Results **64**
C.1 Preliminary Definitions 64
C.2 Simulations 65

D Bessel and Modified Bessel Functions **67**

E Modal Simulations **69**

List of Figures

2.1 A Long Thin Rod Being Heated in a Multizone Furnace 14

3.1 Tubular Reactor for Convection-Diffusion-Reaction Systems 19
3.2 Unforced Profile of $x_{rn}(z,t)$ with Five Modes ($n = 5$). 22
3.3 Forced Solution of $x_r(z,t)$ with $n = 25$. 23
3.4 Concentration Profiles Calculated from Modal Decomposition of $x_r(z,t)$ with $n = 5$ and $n = 25$. 24
3.5 A Distributed Parameter Modal Control Scheme (taken from [Ray, 1981]). 25
3.6 Model Predictive Control: Modal Output and Manipulated Variable Action. 27
3.7 Concentration Output Using Model Predictive Control. 27
3.8 Effect of the Number of Modes on the Error Between the Setpoint and Actual Output (using MPC). 28

4.1 Example Flowsheet of a Bleaching Sequence (taken from [Dence and Reeve, 1996].) 31
4.2 Numerical Integration Results - C_{ss} and its Derivative. 37
4.3 Exponential Model Fit to C_{ss} Data Obtained by Numerical Integration. 38
4.4 Unforced Solution of $\eta_1(z,t)$. 41
4.5 First Value of lambda Satisfying $|B.C.|$=0 48
4.6 Modal Solution of Deviational $\eta_2(z,t)$ (i.e.:$\widetilde{C}(z,t)$) with $n = 5$. 49
4.7 Finite Difference Solution of Deviational $\eta_2(z,t)$ (i.e.: $\widetilde{C}(z,t)$) with a Mesh of 200 Points. 50
4.8 Integral of the Difference Between Finite Difference Method and Modal Method ($n = 5$) Over the Space Variable $'z'$ and the Time Variable $'t'$. 50
4.9 Effect of Varying Number of Modes on "Volume" Difference Beween Finite Difference and Modal Methods. 51

C.1 Setpoint and Actual Output Concentration at Steady State ($t = 55$) using MPC ($n = 5$) at 65
C.2 Setpoint and Actual Output Concentration at Steady State ($t = 55$) using MPC ($n = 10$). 66

D.1 Bessel Functions of the First and Second Kind of Orders 0 and 1. 68

D.2 Modified Bessel Functions of Integer Orders. 68

E.1 Integral of the Difference Between Modal and Finite Difference Solutions for $n = 2, 3, 4$ and 5. 69

E.2 Deviational Chlorine Dioxide Concentration Profiles Using Modal Deomposition for $n = 2, 3, 4, 5$. 70

List of Tables

4.1 Steady State Operating Parameters 36
4.2 First Five Eigenvalues of Linearized Spatial ODE 47

B.1 Finite Difference Approximations 63

D.1 Bessel Functions of the First and Second Kind 67

Chapter 1

Introduction

The chemical process industry is constantly seeking improved control and monitoring methods in order to optimize their operations. As a result, modeling and control of chemical tubular reactors characterized by convection-reaction-diffusion phenomena has been studied to a great extent. Unfortunately, the models describing these systems are distributed in nature: the system variables vary with both space and time, making their analysis mathematically more complicated. This thesis is concerned with the analysis of convection-diffusion-reaction systems using modal decomposition, and its combination with advanced control techniques as well as extension to nonlinear systems.

1.1 Distributed Parameter Systems

There are many industrial processes in which the states, outputs and control variables vary spatially as well as temporally. These processes are known as distributed parameter systems (DPS). The natural form of the models that describe distributed parameter systems are partial differential equations (PDEs), integral equations or trandscendental transfer functions [Ray, 1981]. An example is the one-dimensional heat equation:

$$\frac{\partial T}{\partial t} = \Psi \frac{\partial^2 T}{\partial z^2} \tag{1.1}$$

where T represents the temperature of a heat-conducting rod having Ψ as its thermal diffusivity.

Currently, for simplification and control purposes, most industrial processes are represented by lumped parameter models, which are characterized by ordinary differential equations. However, a large number of these processes are actually distributed in nature, and simple lumped parameter models that ignore the spatially varying nature of the DPS will often suffer from strong interactions and apparent time delays due to the underlying diffusion and convection phenomena inherent in these processes [Gay and Ray, 1995]. Examples such as heat transfer and sheet forming processes, heat exchangers, reactors and bioreactors, are just a few of the many processes where the dependent variables may vary

in space as well as in time. For the purpose of this work, we will concentrate on partial differential equation representations of DPS because they stem from fundamental momentum, energy and material balances for a process. More specifically, we will concentrate on one specific type of PDE: parabolic equations.

Parabolic systems play an important role in the description of the dynamics of chemical processes. Parabolic equations can be used to describe the dynamics of tubular reactors whenever dispersion phenomena are present, as shown in Equation (1.2)[1].

$$\frac{\partial x(z,t)}{\partial t} = -v\frac{\partial x(z,t)}{\partial z} + D\frac{\partial^2 x(z,t)}{\partial z^2} - kx(z,t) \tag{1.2}$$

Typically parabolic equations modeling tubular reactors with axial dispersion can be viewed as a very general case, which is intermediate between the ideal cases: the continuous stirred tank reactor (CSTR) and the plug-flow reactor (PFR). When the diffusion coefficient is large, the distributed parameter parabolic model tends to the lumped parameter model of a CSTR. Conversely, when it is small, the model tends to the (hyperbolic) plug flow reactor model. This phenomenon has been largely analysed in a number of scientific publications (by using for example singular perturbations techniques) like those of Cohen and Poore [1974] and Varma and Aris [1977]. The two extreme cases (CSTR and PFR) rarely occur in practice as there is always some degree of back-mixing in a tubular reactor. It is for this reason that the intermediate axial dispersion model is of great interest, and thus the parabolic PDEs which model these physical systems are the focus of this thesis.

1.2 Control of Distributed Parameter Systems

Research in the field of control of DPS has been ongoing since the 1970's. Ray published a survey of applications of distributed parameter systems theory, which encompassed a large number of fields, indicating a need for further applications research [Ray, 1978]. Dochain [1994] notes that although research in the theory of DPS is still quite active, it faces two problems. The first is related to the high degree of abstraction of DPS: a lot of the research is done by mathematicians who handle rather abstract and complex mathematical objects (the mathematical complexity is due to the infinite dimensionality of DPS). This complexity then makes the connection with practical aspects of industrial process and systems very difficult. The second problem is that most results do not apply to nonlinear DPS [Dochain, 1994].

Analytical solution of partial differential equations describing DPS is generally nontrivial and in many cases impossible [Hanczyc and Palazoglu, 1995]. Due to the mathematical complexity of PDEs, approximation methods have been studied to a great extent. Conventional approaches for control of DPS are based on spatial discretization of the PDE model, yielding a finite number of ordinary differential equations in time [Christofides and Daoutidis, 1996*a*]. The rich theory available for the control of lumped parameter systems can

---

[1] Where v is the superficial fluid velocity, D is the diffusion coefficient, x is the reactant concentration and k is the kinetic constant.

then be applied to the discretized system of ODEs. Unfortunately, common discretization techniques such as finite difference, finite element and finite volume methods often yield large systems of ODEs, making the problems computationally unattractive and losing information contained in the model. Also, notions such as controllability and observability may depend on the discretization method and the number and location of discretization points [Ray, 1981].

Efforts have been made to reduce the number of ODEs necessary to represent the true distributed parameter system. Orthogonal collocation and other weighted residual methods [Villadsen and Michelsen, 1978] can result in systems of lower order. Others use the method of characteristics combined with a sliding mode technique developed by Sira-Ramirez [1989], and further developed by Hanczyc and Palazoglu [1995] and Shang et al. [2000], for hyperbolic PDEs.

For parabolic systems, modal decomposition has often been employed to provide approximate solutions and theoretical results regarding control of DPS [Gay and Ray, 1995]. Murray-Lasso [1965] first presented modal decomposition for DPS in the 1960's, and it was developed to a great extent by Ray [1981]. It is based on the ability to represent the spatially varying input and output of the system as a sum of an infinite series of the system's spatial eigenfunctions and time-dependent coefficients. This is similar to the collocation and weighted residual techniques; however modal analysis has the distinct property that the spatial eigenmode coefficients are decoupled. Motivated by the fact that modal decomposition uses the natural structure of the PDE to solve for the spatial eigenfunctions (which is a property that the above methods do not have), the purpose of this research is to investigate modal decomposition techniques and evaluate them for use in control applications. Modal decomposition will be described in greater detail in Chapters 2-4.

Research in the application of various control techniques to DPS includes the work by Elisante et al. [1999] who designed an IMC-based pole placement controller for modal control of a heat conduction process, and Christofides [1998] who combined Galerkin's method with the design of robust controller via Lyapunov's direct method. However, despite the popularity and remarkable industrial success of Model Predictive Control (MPC), the application of MPC to distributed parameter systems has received very limited attention from both industrial practitioners and academics, alike. Shang et al. [2000] applied Model Predictive Control in combination with the method of characteristics, however there seems to be little in the literature on the application of MPC to distributed parameter systems. One may consult [Bewley, 2001,Bewley and Liu, 1998] for recent research in the field of advanced control of DPS. As a result, modal decomposition was investigated for its potential application to MPC for convection-reaction-diffusion systems.

1.3 Thesis Scope and Objectives

This thesis focuses on the application of modal decomposition to convection-reaction-diffusion DPS. The principle objective is to investigate the use modal decomposition for convection-diffusion-reaction systems in order to convert the DPS to control-relevant forms. As previously mentioned, this method of PDE decomposition was the subject of some research from the late 60's [Murray-Lasso, 1965] to the early 1980's. However, to the author's knowledge, modal decomposition has not been combined with control techniques such as Model Predictive Control, nor has it been the subject of much research in its application to nonlinear systems[2].

As a result, the first main contribution of this thesis is the application of modal decomposition to a linear convection-diffusion-reaction system, combined with a Model Predictive Controller designed in the modal space. It is important to note that it was not the intent of the author to research MPC techniques in depth, but to simply evaluate the use of modal decomposition for use with MPC, as it is often considered the current industrial 'standard' approach to control in the chemical industries.

The second main contribution of the research was an investigation of the application of modal decomposition to an industrial problem (pulp bleaching reactor) modeled by a set of nonlinear PDEs. Although the author was aware of the limitations of the application linear methods to nonlinear systems, a preliminary investigation was done, and promising results are shown. The encouraging results show potential for future use of this method in control applications. A framework for producing the linear tangent model and applying modal decomposition (to make the model amenable for the application of lumped parameter control methods) was developed.

Chapter 2 provides a brief overview of some PDE models, solution techniques, and some of the decomposition methods including modal decomposition. Chapter 3 examines modal decomposition more specifically for convection-diffusion-reaction systems. A case study of tubular reactor with linear reaction kinetics is studied and Model Predictive Control is applied in the modal space. Chapter 4 presents another case study, this time of a practical industrial problem: a nonlinear bleaching reactor model. Modal decomposition is applied to a linear tangent approximation of the bleaching reactor model.

---

[2] For upcoming research in the field, one may consult [Bewley, 2001,Bewley and Liu, 1998].

Chapter 2

Modelling and System Background

Mathematical models describing many physical systems found in the field of chemical engineering are distributed in nature. Although a certain number of these may be approximated by lumped parameter models due to the fact that the distributed parameter aspect is negligible; it is important to keep the distributed nature for some of them (e.g., for tubular reactors, heat diffusion systems,...) [Dochain, 1994]. These DPS cannot be well approximated with lumped parameter systems models (ODEs), and are therefore modeled using partial differential equations. The properties of distributed parameter systems depend strongly on the type of partial differential equations by which they are described. It is therefore necessary to establish some background knowledge in partial differential equations (PDEs) [Ray, 1981].

The goal of this chapter is to introduce the reader to the basic mathematics surrounding PDEs, and to provide an overview of some of the most common solution techniques for each of the different PDE types. The focus will be on second order PDEs, as the study of parabolic second order PDEs are the main object of interest in this research. The first section introduces some basic concepts regarding partial differential equations and their classification. The subsequent three sections detail the main features of each type of PDE and some common solution techniques. The fifth section describes some of the essential components to properly formulate a PDE model. The last sections are dedicated to some general solution techniques, with emphasis placed on the last method: modal decomposition. These last sections should permit the reader to form a comparison basis for the selected solution method (modal decomposition). The interested reader may consult relevant references and Appendix B for more details.

2.1 PDE Classification

A general form for an 'i^{th}' order PDE may be represented as

$$F\left(z_1, z_2, ..z_i, x, \frac{\partial x}{\partial z_1}, \frac{\partial x}{\partial z_2} ..., \frac{\partial^2 x}{\partial z_1 z_2}, ... \frac{\partial^{(i)} x}{\partial z_i^{(i)}} ...\right) = 0 \tag{2.1}$$

where the independent variables are $z_1, z_2, ..z_i$, and the dependent variable is x. The order of Equation (2.1) is given by the highest order partial derivative appearing in the equation. Also, the equation is considered linear if the PDE is algebraically linear in the independent variables and their partial differentials and the coefficients of the variables are functions only of the independent variables. Two subclasses of nonlinear PDEs are semi-linear and quasi-linear. A PDE is semi-linear if all the derivatives occur linearly, but the coefficients depend on z_i; the PDE is quasi-linear if all highest order derivatives occur linearly, with coefficients depending only on $(z_1, z_2 ... z_i,)$ and the lower derivatives of x [McOwen, 1996]. Generally, a first order PDE model for a distributed parameter system may take the following form (note that all first order PDEs are hyperbolic):

$$\frac{\partial x(z,t)}{\partial t} = a_1 \frac{\partial x(z,t)}{\partial z} + a_0 x(z,t) + b_1 u(z,t) \tag{2.2}$$

A second order PDE in which the derivatives of second order occur linearly can be written as:

$$a_2 \frac{\partial^2 x(z,t)}{\partial t^2} + b_2 \frac{\partial^2 x(z,t)}{\partial z \partial t} + c_2 \frac{\partial^2 x(z,t)}{\partial t^2} = d_2 \cdot F\left(\frac{\partial x(z,t)}{\partial z}, \frac{\partial x(z,t)}{\partial t}, x(z,t), t, z\right) \tag{2.3}$$

The independent variables in this case are t and z (time and position), x is a function of the independent variables (t, z), u is the manipulated variable, and $\frac{\partial x}{\partial z}, \frac{\partial^2 x}{\partial z \partial t}$ are the partial derivatives of x. Second order partial differential equations may be categorized into three different types[1]: hyperbolic, elliptic, and parabolic. Equation (2.3) can be classified as one of the three types based on the roots of its characteristic equation, given by:

$$\frac{dz}{dt} = \frac{-b_2 \pm \sqrt{b_2^2 - 4a_2c_2}}{2a_2} \tag{2.4}$$

The discriminant of Equation (2.4) determines the type of PDE [Ray, 1981].

1. $\sqrt{b^2 - 4ac} > 0$, there are 2 real characteristics, and Equation (2.3) is hyperbolic. A common example of this type is the wave equation describing vibrating strings and membranes and sonic and electromagnetic waves.

---

[1] If the coefficients a_2, b_2, c_2, d_2 are not constant, the PDE may change from one type (Parabolic, Elliptic, Hyperbolic) to another depending on the values of these coefficients.

2. $\sqrt{b^2 - 4ac} < 0$, there are no real characteristics, and Equation (2.3) is elliptic. Laplace's equation which describes steady state solutions to the wave and heat equations is elliptic.

3. $\sqrt{b^2 - 4ac} = 0$, there is only one distinct characteristic, and Equation (2.3) is called parabolic. The heat equation and problems involving diffusion are parabolic.

The following three subsections will be devoted to a brief overview of solution methods for each type of PDE.

2.2 Hyperbolic PDEs

As previously mentioned, all first order PDEs are hyperbolic. Moreover, all higher order hyperbolic PDEs may be reduced to system of first order hyperbolic PDEs. First order hyperbolic equations can occur as direct models of physical processes or as approximations to higher order equations or system of equations. For instance, the wave equation (2.5):

$$\frac{\partial x(z,t)}{\partial t} + \alpha_T \frac{\partial x(z,t)}{\partial z} = 0 \tag{2.5}$$

is an approximation to the diffusion (or heat) equation when the diffusion coefficient is negligibly small [Zauderer, 1989]. In chemical engineering applications, hyperbolic PDEs arise in processes such as heat exchangers, chemical reactors and other tubular processes where there is no diffusive term, or the diffusion term is negligible. Second order hyperbolic PDEs occur in wave propagation.

Solution Approaches

Laplace transforms can be used to solve linear hyperbolic PDEs. The main drawbacks to using this method is that it is only applicable to linear systems, and difficulty may arise in the inversion of the transforms back to the original state [Ray, 1981]. Another method commonly used for hyperbolic PDEs is the method of characteristics. The method of characteristics is useful in control applications, as the PDE can exactly be described by a set of ODEs along its characteristic curves. The reader may consult Appendix B for further review of this method.

2.3 Elliptic PDEs

Elliptic PDEs occur in multidimensional diffusion or heat transport problems such as steady state conduction in a two-dimensional slab [Ray, 1981]:

$$\alpha_T \left(\frac{\partial^2 T}{\partial z^2} + \frac{\partial^2 T}{\partial y^2} \right) = 0 \tag{2.6}$$

This is also known as Laplace's equation in two dimensions. In general, elliptic equations involving *time* and a spatial variable rarely occur because physical systems can seldom (if ever) be represented by these modeling equations [Ray, 1981]. This research is concerned with distributed parameter systems varying in time and space, therefore we will not place great emphasis on solution approaches to elliptic PDEs since they represent steady-state systems.

2.4 Parabolic PDEs

Representative examples of industrial processes described by parabolic PDEs include fluidized beds, packed beds, and other tubular reactors [Georgakis and Amundson, 1977; Christofides and Daoutidis, 1996*b*], thermal regenerators (blast furnaces) and other heat treatment applications [Christofides, 1998].

Solution Approaches

Common approximation methods include Galerkin's method, orthogonal collocation, and modal analysis. Galerkin's method approximates the infinite dimensional state with a truncated series representation.

$$x(z,t) \approx \sum_{i=1}^{n} c_i(t)\,\beta_i(z) \tag{2.7}$$

where $[\beta_i(z) ... \beta_n(z)]$ are the elements of a smooth, complete, orthonormal set [Hanczyc and Palazoglu, 1992]. Substituting this series approximation into the original PDE yields a finite dimensional ODE representation of the system. Sadek et al. [1998] explain that this approach approximates the state and/or control by finite-term series whose coefficient values are to be determined optimally. Typical examples of the basis functions ($\beta_i(z)$) used are Chebyshev polynomials, Laguerre polynomials, Legendre polynomials, Fourier and Taylor series, and others found in Sadek et al. [1998]. A more detailed discussion of these solution methods is found in Section 2.6.

2.5 Model Requirements for Problem Formulation

The previous section discussed classification and solution approaches to partial differential equation models. These solution methods produce general solutions to PDEs. However, in most cases, we are not merely interested in finding arbitrary functions that satisfy the given differential equation; rather we seek specific solutions that satisfy certain conditions associated with a given physical problem [Zauderer, 1989]. For example, the heat and wave equations are of parabolic and hyperbolic types, respectively; and both contain a time dependence. It is therefore often appropriate to assign values to the solutions at an initial time $t = 0$. In the case, where the value of z (the spatial variable) is unrestricted, an

initial value problem is formed. However, when the values of z are restricted to lie in a bounded or semi-infinite interval, then $x(z,t)$, $\frac{\partial x}{\partial t}$, or some linear combination of both must be prescribed on some boundary for all $t \geq 0$. This constitutes an *initial and boundary value problem* [Zauderer, 1989]. Laplace's Equation (2.6) was shown to characterize a steady state situation where no time dependence plays a role, therefore the unknown function ($T(z,y)$ in the case of Equation (2.6)) would be specified on the boundary of the region under consideration. This is considered to be a *boundary value problem* for Laplace's equation.

The number of initial and/or boundary conditions that should be assigned for a given PDE depends on many factors; and the problem of deciding what form of initial and/or boundary data are necessary for a given PDE is complicated [Zauderer, 1989]. A set of guidelines was proposed by Hadamard [cf., Zauderer, 1989]. He listed three requirements that must be met in order for the problem to be *well posed.* The three conditions are:

1. At least one solution must exist,
2. The solution must be unique (there must be at most one solution),
3. The solution must depend continuously on the initial and/or boundary data.

If a mathematical model satisfies all three criteria of existence, uniqueness and continuity, the problem is said to be *well posed.* The problems that will be addressed in this thesis are sufficiently standard that their appropriate formulations are well understood, and it is known that they are well posed. Nevertheless, one must be aware that any PDE representing a physical process may have been obtained under various assumptions and simplifications, and it is not always a priori obvious that the formulation is well posed [Zauderer, 1989].

2.6 General Solution Methods

Solutions of PDEs can take several forms. They may take classical forms, in which the unknowns are described in the solution explicitly by some mathematical expression as continuous function of the independent variables. This form is called the closed-form solution. [Street, 1973]. The mathematical functions are typically infinite series, power series and/or other combinations of functions. It it not very often, however, that a PDE is simple enough so that a closed form solution may be found. One then tends to look to numerical computation methods, or numerical solutions obtained by approximation techniques. Some of these numerical methods, as well as some closed-form solution methods will be addressed in the following subsections.

2.6.1 Finite Difference Approximations

Some mathematical models are too complex to be able to find a solution of closed from. As previously mentioned, one must then look to numerical solution techniques in order to

approximate model solutions. The method of finite differences is universally applicable to linear and nonlinear systems regardless of the domains or inhomogeneities involved [Street, 1973].

In finite difference approximations, the derivatives of functions are replaced by their corresponding difference quotients stemming from Taylor series approximations [Street, 1973]. There are several difference approximations that may be used. One of the considerations that is taken into account when selecting which difference scheme to use is the numerical stability of the solution. Instability occurs when the difference equation admits an exponentially growing solution that rapidly masks the true solution to the differential equation [Street, 1973]. One may refer to Appendix B for more detail on this topic.

2.6.2 Numerical Techniques Using Weighted Residual Methods (WRM)

Orthogonal collocation and finite elements are part of the family of the *methods of weighted residuals* (abbreviated WRM in the literature for weighted residual methods). They are techniques for developing approximate solutions of partial differential equations. Both collocation and finite elements use the idea that the unknown solution is approximated by a set of local basis functions containing adjustable constants or functions. These constants or functions are chosen using various criteria to give the 'best' approximation for the solution [Ames, 1977].

Re-iterating Equation (2.7), the solution to a PDE may be expressed as:

$$\widetilde{x}(z,t) \approx \sum_{i=1}^{n} c_i\,(t)\,\beta_i\,(z) \tag{2.8}$$

The constants or functions $c_i(t)$ are chosen in such a way that the residuals (R_e) are minimized over the domain Ω. These residuals are a measure of how well the trial function $\widetilde{x}(z,t)$ satisfies the partial differential equation and the initial conditions [Ames, 1977]. The weighting functions, w_i are chosen such that

$$\int_{\Omega} R_e w_i d\Omega = 0 \tag{2.9}$$

The methods of weighted residuals differ from one another because of the choice of the weighting functions w_i.

Orthogonal Collocation

As for any orthogonality WRM, the weighting functions in orthogonal collocation are chosen so as to be orthogonal to the residual. More specifically, these are chosen to Dirac delta distributions:

$$w_i = \delta(z - z_i) \tag{2.10}$$

This gives the following relationship for the residual:

$$\int_{\Omega} R_e \delta(z - z_i) d\Omega = R_e(z_i) = 0 \tag{2.11}$$

(i.e., the residual is equal to zero at the *collocation* points z_i.)

In practice, the first step in orthogonal collocation consists of writing the finite expansion of each state variable as a weighted sum of their values at the collocation points:

$$x(z,t) \cong \sum_{i=0}^{q} \beta_i(z) x_i(t) \tag{2.12}$$

where the basis functions $\beta_i(z)$ are as *orthogonal* functions with:

$$\beta_i(z = z_j) = \delta_{ij} \tag{2.13}$$

and $x_i(t)$ are the values of $x(z,t)$ at the position (collocation point) $z = z_i$:

$$x_i(t) = x(z = z_i, t) \tag{2.14}$$

The second step consists of rewriting the spatial derivatives by considering the above Equation (2.12), i.e.:

$$\frac{\partial x}{\partial z} \cong \sum_{i=0}^{q} \frac{d\beta_i(z)}{dz} x_i(t) \tag{2.15}$$

$$\frac{\partial^2 x}{\partial z^2} \cong \sum_{i=0}^{q} \frac{d^2\beta_i(z)}{dz^2} x_i(t) \tag{2.16}$$

These two steps allow the PDE in the variable $x(z,t)$ to be approximated by a finite number of ODEs for each $x_i(t)$. The implementation requires the choice of the basis functions $\beta_i(z)$, and the number and position of the collocation points [Michelsen and Villadsen, 1972]. The most widely used basis functions are the Lagrange polynomials:

$$\beta_i(z) = \prod_{j=0, \neq i}^{q} \frac{z - z_j}{z_j - z_i} \tag{2.17}$$

The collocation points are usually computed as zeros of orthogonal polynomials, among which Legendre and Jacobi polynomials are typically the most largely used. It has been shown in Lefevre et al. [2000] that the choice of Jacobi polynomials corresponds to an optimal choice with respect to an non-uniform norm. This implies that the discretization points may be distributed non-uniformly with (for example) more points concentrated close to hot spots or points for which some state variables are characterized by large variations.

Finite Elements - Bubnov-Galerkin method

In using the finite element method, the domain Ω is partitioned into a large number of subdomains called elements. The local representation of the PDE solution is then the form of the approximate solution in an individual element [Gladwell and Wait, 1979]. Not unlike orthogonal collocation, the solution can be expressed as a sum of basis functions. However, in the Bubnov-Galerkin method, the weighting functions w_i are chosen to be the basis functions of the trial solution [Ames, 1977].

$$w_i = \beta_i \tag{2.18}$$

This has the advantage that the residual is made orthogonal to each basis function and is, therefore the best possible solution made up of the N functions β_i. Therefore as $N \to \infty$, $R_e \to 0$ because it will be orthogonal to every function in a complete set of basis functions [Ray, 1981]

Method of Subdomains.

The method of subdomains is another WRM with the weighting functions chosen to be a set of Heaviside functions breaking the domain into subdomains. For example, if the spatial domain were $0 \leq z \leq 1$ [Ames, 1977]:

$$w_i = \begin{cases} 1 & z_n < z < z_{n+1} \\ 0 & \text{elsewhere} \end{cases} \tag{2.19}$$

Method of moments

This method was originally developed to study nonlinear diffusion and laminar boundary layer problems [Ames, 1977]. For a PDE in one spatial variable z, the weighting functions are chosen to be powers of z:

$$w_i = z^i \tag{2.20}$$

2.7 Modal Decomposition

The previous sections showed various methods to decompose a PDE using a set of basis functions. In all these cases, the basis functions were chosen somewhat arbitrarily to serve one purpose: create a lumped parameter system which is a good approximation of an infinite dimensional system. Modal decomposition, (sometimes referred to as modal analysis) is a specific case of basis function decomposition, where the basis functions are the eigenfunctions of the PDE. The lumping methods shown in the previous section can be

thought of as "pseudo modal methods", where one may use any set of basis functions and a goodness-of-fit criterion to decompose the PDE. However modal decomposition uses the eigenfunction expansions of the linear operator [Ray, 1978].

Modal analysis can also be seen as a specific case of Galerkin's method, where the basis functions are chosen to be the eigenfunctions of the system. However, it is important to know that Galerkin's method differs from exact modal analysis in that the solution to the PDE system using Galerkin's method is only approximate and the smallness of the residual R_e will depend on the *type* and number of basis functions chosen. Modal decomposition uses the actual structure of the PDE and the error in the solution stems only from the fact that we are unable to sum an infinite number of terms in the series. This decomposition method uses the technique of eigenfunction expansion to reduce the DPS model to a set of ODEs which are fully decoupled in terms of eigenvalues [Elisante and Matsumoto, 1999*a*].

Modal analysis is a technique not only used in distributed parameter systems, in fact it was first used for lumped parameter systems, then extended to DPS in the 1960's by Murray-Lasso [1965] (cf., Gould [1969]). The central theme behind modal analysis is that the dynamic behavior of a system is predominantly determined by the modes associated with the smallest (or slowest) eigenvalues. If it is possible to approximate a high order system by a lower-order system whose slow modes are the same as those of the original system, then attention can be given to the eigenvalues of the slow modes [Gould, 1969]. Modal decomposition is an attractive method of treating PDEs which have a real, discrete spectrum of eigenvalues. It is a natural reduction technique and works especially well when a few modes accurately capture all important dynamics [Ray, 1978]. Modal decomposition is often well suited for parabolic PDEs. A particularly successful example from the literature is the heat equation; it will be used to illustrate modal decomposition in Section 2.7.1.

2.7.1 Parabolic Example: Heat Equation

The following parabolic PDE represents the heat distribution along a uniform rod heated in a multizone furnace in order to achieve a desired temperature distribution. Fig (2.1) depicts the physical situation (taken from Ray, 1981).

Note this model is very similar to Equation (1.1).

$$\frac{\partial T}{\partial t} = \Psi \frac{\partial^2 T}{\partial z^2} + Q(z,t) \tag{2.21}$$

where

$$\Psi = \frac{k_T}{\rho_d C_p}. \tag{2.22}$$

Ψ is the thermal diffusivity, ρ_d is the material density, k_T is the thermal conductivity, and C_p is the specific heat of the material. This example is treated in both [Ray, 1978] and [Gould, 1969]. The heaters provide a heat flux distribution $Q(z,t)$ that is adjustable in both time

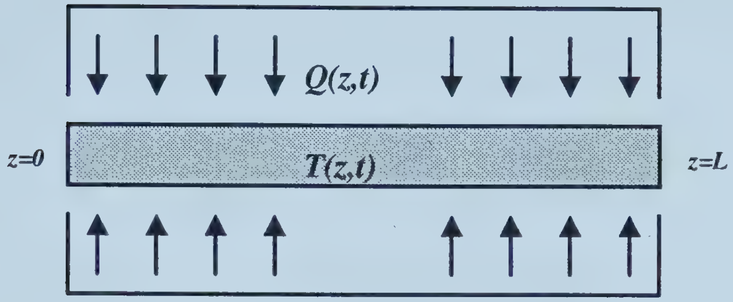

Figure 2.1: A Long Thin Rod Being Heated in a Multizone Furnace

and spatially along the rod. In the absence of heaters, the temperature distribution would decay to a steady state. The state (temperature) at any instant of time t, is determined by $T(z,t)$, which is generally a continuous function of distance 'z'. The task is to represent this infinite dimensional state in a more convenient way. Conventionally, this is done by partitioning the system into N parts (i.e., using finite differences) where the temperature in each partition is the mean value of the temperature within that partition. Unfortunately this approach is not the most efficient way to approximate the state, particularly if one is interested in the slowest modes [Gould, 1969].

Assuming that there is no heat loss at the ends of the rod, the boundary conditions are

$$\frac{\partial T(0,t)}{\partial z} = \frac{\partial T(1,t)}{\partial z} = 0 \tag{2.23}$$

with an initial condition

$$T(z,0) = T_0 \tag{2.24}$$

One can put the variables in dimensionless form:

$$\begin{aligned} \widehat{t} &= t\Psi \\ \widehat{z} &= z \\ u(\widehat{z},\widehat{t}) &= \frac{Q(z,t)l^2}{k_T T_0} \\ x(\widehat{z},\widehat{t}) &= \frac{T(z,t)}{T_0} \end{aligned} \tag{2.25}$$

For convenience, the $\hat{}$ will be omitted, however it is understood that the variables are in dimensionless form by Equation (2.25). Noting that Equation (2.21) and Equation (2.23) form a parabolic model with homogenous boundary conditions that is amenable to separation of variables. We assume the solution is of the form:

$$x(z,t) = \sum_{n=0}^{\infty} a_{Tn}(t)\,\phi_{Tn}(z) \qquad n = 0, 1, 2... \tag{2.26}$$

where the a_{Tn} and ϕ_{Tn} are temporal and spatial functions (respectively) to be determined. The subscript T indicates that the functions are those associated with the temperature distribution. (It is necessary to use the subscripts, as these same variables will be used in Chapter 3 for the modal decomposition of concentration in a tubular reactor model).

The input, $u(z,t)$,can be expanded in the same manner

$$u(z,t) = \sum_{n=0}^{\infty} b_{Tn}(t)\,\phi_{Tn}(z) \tag{2.27}$$

Introducing Equation (2.26) and (2.27) into Equation (1.1) yields:

$$\frac{da_{Tn}(t)}{dt}\phi_{Tn}(z) = \frac{d^2\phi_{Tn}(z)}{dz^2}a_{Tn}(t) + b_{Tn}(t)\,\phi_{Tn}(z) \tag{2.28}$$

Dividing Equation (2.28) by $a_{Tn}(t)\,\phi_{Tn}(z)$ yields a set of ODEs which may be divided into a left side which depends solely on t and a right side which is a function of z alone. For this equality to hold for all (z,t), both sides of the equation must be equal to a constant λ_{Tn}.

$$\frac{1}{a_{Tn}(t)}\left[\frac{da_{Tn}(t)}{dt} - b_{Tn}(t)\right] = \frac{1}{\phi_n(z)}\left[\frac{d^2\phi_{Tn}(z)}{dz^2}\right] = \lambda_{Tn} \tag{2.29}$$

Equation (2.29) can then be separated into the following ODEs that formulate the eigenvalue problem

$$\frac{d^2\phi_{Tn}(z)}{dz^2} - \lambda_{Tn}\phi_n(z) = 0 \qquad n = 0, 1, 2... \tag{2.30}$$

$$\frac{da_{Tn}(t)}{dt} - \lambda_{Tn}a_{Tn}(t) = b_{Tn}(t) \qquad n = 0, 1, 2.... \tag{2.31}$$

Equation (2.30) is a second order linear ODE with constant coefficients whose general solution is given by

$$\phi_{Tn}(z) = C_1\cos\left(\sqrt{\lambda_{Tn}}z\right) + C_2\sin\left(\sqrt{\lambda_{Tn}}z\right) \tag{2.32}$$

On application of the boundary conditions, one obtains

$$\phi_{Tn}(z) = A_{Tn}\cos\left(\sqrt{\lambda_{Tn}z}\right) \tag{2.33}$$

and the λ_{Tn}, are found by solving Equation (2.34)

$$\sqrt{\lambda_{Tn}}\sin\sqrt{\lambda_{Tn}} = 0 \tag{2.34}$$

The only possible solutions to this are

$$\sqrt{\lambda_{Tn}} = n\pi$$

or

$$\lambda_{Tn} = n^2\pi^2 \tag{2.35}$$

Here the λ_{Tn} are the *eigenvalues* of the system and $\phi_{Tn}(z)$ are the *eigenfunctions* of the system.

Using the properties of orthogonal functions and Sturm-Liouville theory, the A_{Tn} coefficients are chosen such that $\|\phi_{Tn}\|_2 = 1$ [Ray, 1981],[Renou, 2000]

$$(A_{Tn})^2 = \left[\int_0^1 \left(\cos\sqrt{\lambda_{Tn}z}\right)^2 dz\right]^{-1} \tag{2.36}$$

$$A_{Tn} = \begin{cases} 1 & n = 0 \\ \sqrt{2} & n = 1, 2, ... \end{cases} \tag{2.37}$$

The original distributed parameter system Equation (2.21) has now been decomposed into a set of n ODEs characterized by the system's eigenfunctions, ϕ_{Tn} and its eigenvalues, λ_{Tn}.

The above example showed an example where the parabolic PDE model was decomposed along its eigenfunctions. The eigenfunctions, in this case stemmed from the solution of a linear second order differential equation. The second order differential operator defined over the region $0 < z < 1$ was, in this case[2]:

$$L(\cdot) = a\frac{d^2(\cdot)}{dz^2} \tag{2.38}$$

---

[2] In this example, the differential operator was already *self-adjoint* (see Appendix A for further details and [Ray, 1981]). Self adjoint operators have some nice properties which will be seen later in Chapter 3. Modal analysis does not always lead to self-adjoint operators for the spatial ODE. However it is possible to perform a change of variable in order to make the operator self-adjoint.

2.8 Summary

This chapter introduced the basic mathematics surrounding PDEs, and provided an overview of some of the most common solution techniques for each of the different PDE types. The main focus was on second order PDEs, as the study of parabolic second order PDEs is the main object of interest in this research. Some general solution techniques were shown, with emphasis placed on the chosen method: modal decomposition. These other methods were shown to permit the reader to form a comparison basis for the selected solution method (modal decomposition). It is important to note that modal decomposition is the only method that uses basis functions that are not chosen arbitrarily, but in fact stem from the natural structure of the PDE. Modal decomposition was shown to be a potentially useful method (for parabolic PDEs) for representing an infinite dimensional system as a low dimensional lumped parameter system with few modes. If physical systems are amenable to modal decomposition, then once a lumped parameter system is obtained using this method, it is possible to use conventional control methods to design controllers in the lumped parameter space. The following chapter investigates how an important class of parabolic systems (convection-reaction-diffusion systems) may benefit from modal analysis, and how a MPC controller may be designed in this modal space.

Chapter 3

Modal Decomposition for Parabolic Diffusion-Reaction Systems

Modal decomposition was briefly introduced in Chapter 2 with the heat equation example. The main focus of this research, however, is the application of this method to convection-reaction-diffusion systems. These systems typically describe tubular chemical reactors. Although research has considered non-adiabatic models (e.g., Georgakis and Amundson, [1977]), this thesis examines only isothermal tubular reactors. This chapter is dedicated to modal decomposition specifically for convection-reaction-diffusion systems. We first look at the parabolic operator that describes these reactors, and then proceed to show the steps required to make these models amenable to modal decomposition[1].

An example is considered with one reactant and linear reaction kinetics. To show potential application of this lumping method, a Model Predictive Controller is designed in the new modal space. Promising results are shown with the design of the Model Predictive Controller using just five modes. The results are encouraging and merit further investigation into the application of modal decomposition to DPS to produce lumped parameter models usable for controller design.

3.1 Convection-Diffusion-Reaction Model

A tubular reactor is depicted in Figure 3.1. Often these reactors are fed at the inlet boundary ($z = 0$) with a certain reactant concentration (x_r) in order to obtain a desired outlet product concentration at ($z = l$). As a result, the input ($x_{r,in}$) appears in the boundary condition of the model. The first step in rendering the model amenable to modal decomposition is to make the boundary conditions homogenous. Following this, a similar method to the one shown in Chapter 2 is used for the modal decomposition. The method of separation of variables is used, and the spatial ODE is solved using some of the mathematical tools

---

[1] A brief introduction to adjoint and self-adjoint operators may be found in Appendix C. It is not the intention of the author to enter into all the details of linear operator theory; only to discuss some of the tools required to employ modal decomposition for these parabolic PDE models.

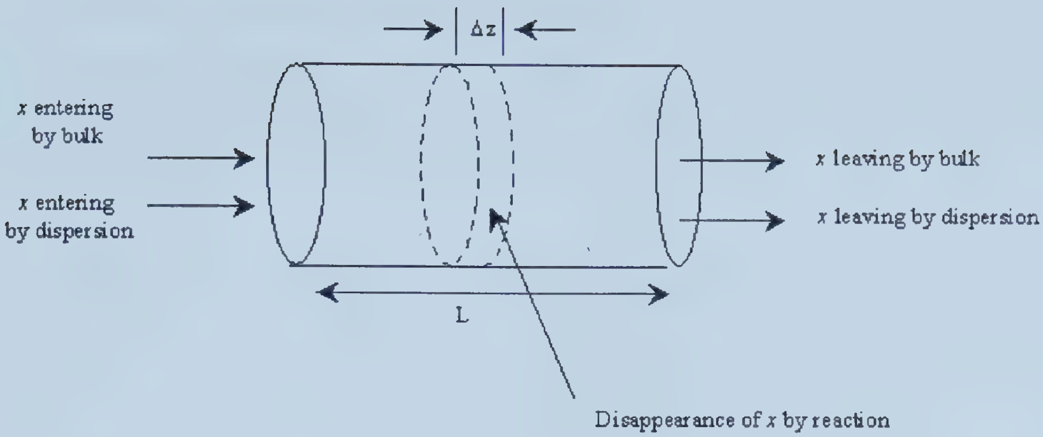
Δz
x entering by bulk
x entering by dispersion
x leaving by bulk
x leaving by dispersion
L
Disappearance of x by reaction

Figure 3.1: Tubular Reactor for Convection-Diffusion-Reaction Systems

discussed in Section 2.1.

3.1.1 Model with linear reaction kinetics

The linear parabolic PDE model shown by Equation (3.1) represents a reaction with a single reactant x_r occurring in a tubular reactor (see Figure 3.1) with axial dispersion and first order reaction kinetics.

$$\frac{\partial x_r(z,t)}{\partial t} = -v\frac{\partial x_r(z,t)}{\partial z} + D_r\frac{\partial^2 x_r(z,t)}{\partial z^2} - k_r x_r(z,t) \tag{3.1}$$

Danckwerts boundary conditions[2] are:

$$D_r\frac{\partial x_r(0,t)}{\partial z} = v\left(x_{r,in}(t) - x_r(0,t)\right) \tag{3.2}$$

$$\frac{\partial x_r(l,t)}{\partial z} = 0 \tag{3.3}$$

with initial condition:

$$x_r(z,0) = x_{r,0}(z)$$

where x_r is the reactant concentration , z is spatial position (m), v is the superficial fluid velocity (m/s), k_r is the kinetic constant $(1/s)$, D_r is the diffusivity, and l is the reactor length (m).

---

[2] The use of Danckwerts boundary conditions has been the topic of much discussion. One may consult [Aris, 1999; Pearson, 1959] for justification of their use in modeling reactors.

3.1.2 Converting inhomogeneous boundary conditions

In order to render the boundary conditions homogenous, Equation (3.2) is combined with Equation (3.1) using the delta Dirac distribution, $\delta(z)$. Ray [1981] demonstrates that Equation (3.4)-(3.6) are equivalent to the original model.

$$\frac{\partial x_r(z,t)}{\partial t} = -v\frac{\partial x_r(z,t)}{\partial z} + D_r\frac{\partial^2 x_r(z,t)}{\partial z^2} - k_r x_r(z,t) + \delta(z)x_{r,in}(t) \tag{3.4}$$

$$D_r\frac{\partial x_r(0,t)}{\partial z} - v x_r(0,t) = 0 \tag{3.5}$$

$$\frac{\partial x_r(l,t)}{\partial z} = 0 \tag{3.6}$$

3.1.3 Modal decomposition

Equation (3.4) with its homogenous boundary conditions is now amenable to separation of variables. As in Chapter 2, we assume the solution is of the form:

$$x_r(z,t) = \sum_{n=0}^{\infty} a_{rn}(t)\,\phi_{rn}(z) \tag{3.7}$$

The input, $x_{r,in}(t)$, can be expanded in the same manner (note that the input can vary in both space and time as well, however for this example, it is a function of t only).

$$\delta(z)x_{r,in}(t) = \sum_{n=0}^{\infty} b_{rn}(t)\,\phi_{rn}(z) \tag{3.8}$$

Introducing Equation (3.7) and (3.8) into Equation (3.4) results in Equation (3.9):

$$\begin{aligned}\frac{da_{rn}(t)}{dt}\phi_{rn}(z) &= -v\frac{d\phi_{rn}(z)}{dz}a_{rn}(t) + D_r\frac{d^2\phi_{rn}(z)}{dz^2}a_{rn}(t) \\ &\quad -k_r\phi_{rn}(z)\,a_{rn}(t) + b_{rn}(t)\,\phi_{rn}(z)\end{aligned} \tag{3.9}$$

Dividing Equation (3.9) by $a_{rn}(t)\,\phi_{rn}(z)$ yields an ODE which may be divided into a left side which depends solely on t and a right side that is a function of z alone. For this equality to hold for all (z,t), both sides of the equation must be equal to a constant. Combining this constant with k_r, and naming it λ_{rn} yields:

$$\frac{1}{a_{rn}(t)}\left[\frac{da_{rn}(t)}{dt} - b_{rn}(t)\right] = \frac{1}{\phi_{rn}(z)}\left[-v\frac{d\phi_{rn}(z)}{dz} + D_r\frac{d^2\phi_{rn}(z)}{dz^2}\right] = \lambda_{rn} \tag{3.10}$$

Equation (3.10) can then be separated into the following ODEs that formulate the eigenvalue problem:

$$\frac{d^2\phi_{rn}(z)}{dz^2} - v\frac{d\phi_{rn}(z)}{dz} + \lambda_{rn}\phi_{rn}(z) = 0 \tag{3.11}$$

$$\frac{da_{rn}(t)}{dt} + \lambda_{rn}a_{rn}(t) = b_{rn}(t) \tag{3.12}$$

Equation (3.11) is a second order linear ODE with constant coefficients whose general solution is given by:

$$\phi_{rn}(z) = C_1 e^{\frac{v}{2D_r}z}\cos\left(\frac{s_{rn}}{2D_r}z\right) + C_2 e^{\frac{v}{2D_r}z}\sin\left(\frac{s_{rn}}{2D_r}z\right) \tag{3.13}$$

where:

$$s_{rn} = \sqrt{v^2 - 4D_r\lambda_{rn}}$$

On application of the boundary conditions, the eigenvalues, λ_{rn}, are found by solving Equation (3.14):

$$\tan\left(\frac{l}{2D_r}s_{rn}\right) = -\frac{s_{rn}^2 + v^2}{4D_r} - k_r \tag{3.14}$$

The solution is then given by[3]:

$$\phi_{rn}(z) = K_{rn}e^{\frac{v}{2D_r}z}\left[\cos\left(\frac{s_{rn}}{2D_r}z\right) + \frac{v}{s_{rn}}e^{\frac{v}{2D_r}z}\sin\left(\frac{s_{rn}}{2D_r}z\right)\right] \tag{3.15}$$

3.1.4 Simulation Examples

To see the effect of the number of modes on the solution, two simulations were done. The first simulation shows the unforced ($b_{rn}(t) = 0$) solution from a non-zero initial condition $x_{r,0}(z) = 1$.

The temporal ODE given by Equation (3.12) is solved using the initial condition calculated by:

$$a_{rn,0} = \int_0^1 \rho(z)x_{r,0}(z)\phi_n(z)dz \tag{3.16}$$

---

[3] Using the properties of orthogonal functions and Sturm-Liouville theory, the K_{rn} coefficients are chosen such that $\|\phi_{rn}\|_2 = 1$. It is important to note, however, that the differential operator in Equation (3.11) is a non self-adjoint Sturm-Liouville operator with $\rho(z) = e^{-\frac{v}{D_r}z}$ and $\mu(z) = D_r\rho(z)$; therefore we must use Equation (C.6) when finding the K_{rn} coefficients [Ray, 1981],[Renou, 2000].

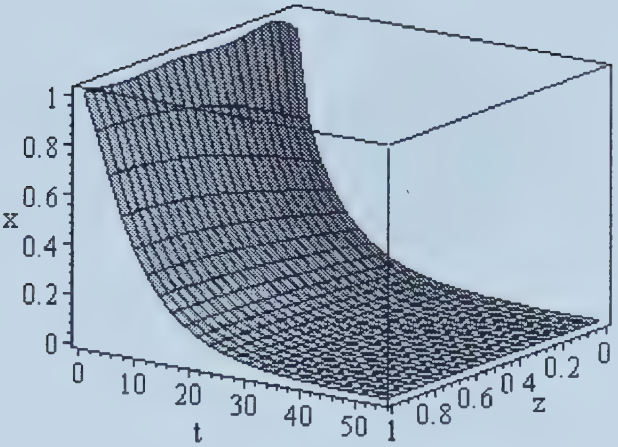

Figure 3.2: Unforced Profile of $x_{rn}(z,t)$ with Five Modes $(n = 5)$.

where:

$$\rho(z) = e^{-\frac{v}{D_r}z} \tag{3.17}$$

The solution to Equation (3.12) is then given by

$$a_{rn}(t) = a_{rn,0}e^{\lambda_{rn}t} \tag{3.18}$$

The first five eigenvalues are $\lambda_{rn} = [-.1156, -.6581, -2.1420, -4.6102, -8.0648]$. Figure 3.2 depicts the solution with only five modes $(n = 5)$. One can see from Figure 3.2 that initially there are small ocsillations in the solution (across the reactor in 'z'), but then the solution progresses smoothly from its initial value of $x_{r,0}(z) = 1$ down to zero. The difference between the unforced solution with $n = 5$ and $n = 25$ is negligible over the entire time span (integral of the absolute error at $t = 55$ is of the order of 10^{-12}). The forced solution is found by using a similar procedure as in the unforced case, but we begin with an initial condition of $x_{r,0}(z) = 0$ and an input $x_{r,in}(z) = 1$. Therefore $b_{rn}(t)$ is calculated by:

$$b_{rn}(t) = \int_0^1 \rho(z)\delta(z)x_{r,in}(z)\phi_n(z)dz \tag{3.19}$$

where $\rho(z)$ is once again given by Equation (3.17). Figure 3.3 depicts the solution surface with $n = 25$. If only five modes are used, the forced solution shows signs of the *sin* and *cos* oscillations from using too few modes. This is shown in Figure 3.4 where a plot of the solution at steady state $(t = 55)$ compares the forced solution with five and twenty five modes.

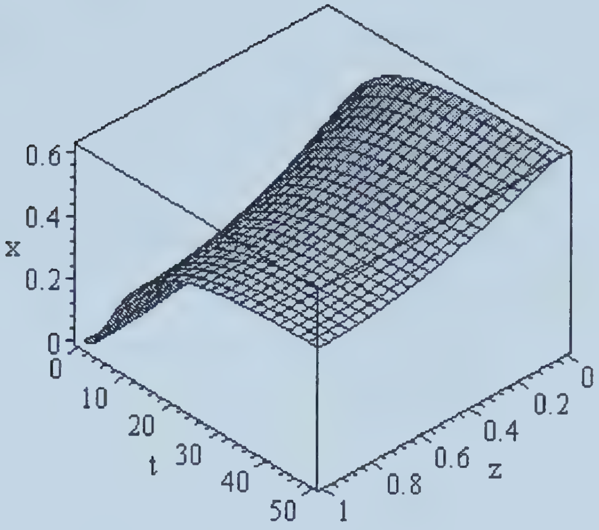

Figure 3.3: Forced Solution of $x_r(z,t)$ with $n = 25$.

From the above sections, it can be concluded that is it is possible for a small number of modes to capture the behaviour of the system, and thus we may be able to represent the infinite dimensional system as a low dimensional lumped parameter system and use conventional control methods.

The original distributed parameter system, Equation (3.1), has now been decomposed into a set of n ODEs characterized by the system's eigenfunctions, ϕ_{rn} and its eigenvalues, λ_{rn}. If the infinite dimensional system can be represented by this finite dimensional approximation, it is then possible to apply conventional control techniques in this new modal space. The following section demonstrates an example of this application with the use of Model Predictive Control in the modal space to achieve a desired profile in the reactor.

3.2 Application Example - MPC in the modal space

Model Predictive Control (hereafter MPC) awareness and interest began in earnest with the publications of papers by Richalet et al. [1978], and Cutler and Ramaker [1979]. However, MPC concepts predate these publications by about 20 years [Ogunaki and Ray, 1994]. The development of MPC was due to the need for better control techniques in industry. In the chemical process and allied industries, the drive for consistent high product quality, more efficient use of energy and increasing awareness of environmental responsibility have created a demand for better performance of control systems than can be met by traditional techniques. The response to this demand, was the development of the industrially successful *Dynamic Matrix Control* (DMC), *Model Algorithmic Control* (MAC) and so forth. These control strategies can be more broadly classified under Model Predictive Control (MPC)

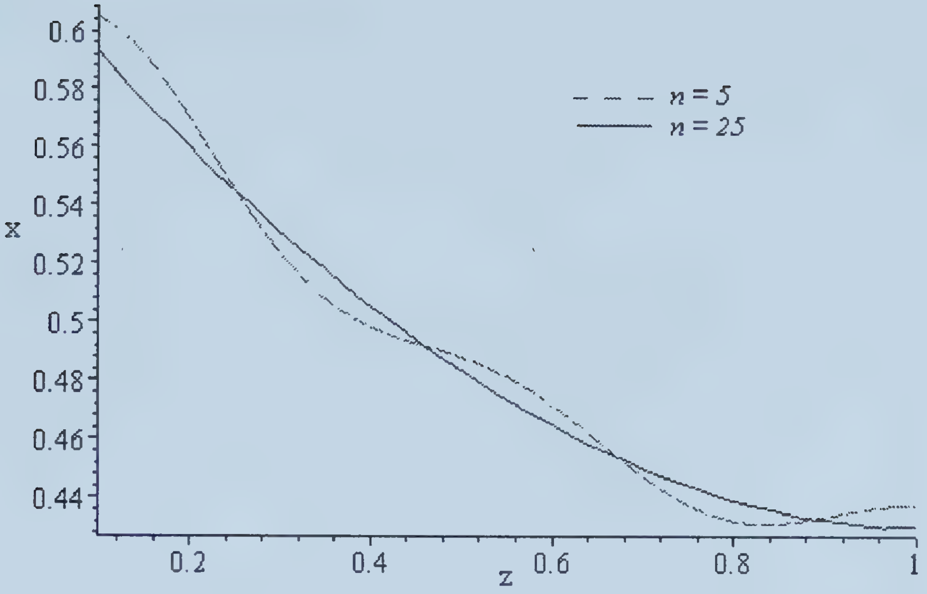

Figure 3.4: Concentration Profiles Calculated from Modal Decomposition of $x_r(z,t)$ with $n=5$ and $n=25$.

schemes.

The essence of Model Predictive Control techniques is, with the use of a process model, to perform two key tasks:

1. predict future plant behavior (over the prediction horizon, p) based on past control actions,
2. compute the optimal control action (over the control horizon, m) to drive the predicted output toward the specified setpoint trajectory.

The most typical model forms used in the design of MPC are step or impulse response models, discrete state space, and transfer function models (see Ogunnaike [1994] for more detail). Normally, the model inputs and outputs are real process variables such as temperature, level, and so on. In this case, the MPC controller will be designed based on a model in the *modal space*; and thus the inputs and outputs are not physical states, but *modal states* (calculated using Equation (3.22)). The model that will be used is a state space model obtained from the modal decomposition in Section 3.2.3 (shown by Equation (3.12)). The modal states in this case are the time varying coefficients of the modal expansions (a_n's) and the $\mathbf{A}$ matrix of the state space model:

$$\dot{\mathbf{x}} = \mathbf{A}\mathbf{x} + \mathbf{B}\mathbf{u} \tag{3.20}$$

which has the eigenvalues on the diagonal:

$$\begin{aligned}\mathbf{x} &= [a_{r1}...a_{rn}] \\ \mathbf{u} &= [b_{r1}...b_{rn}] \\ \mathbf{A} &= diag(\lambda_{rn})\end{aligned} \tag{3.21}$$

Controller design is then done in this new space where the error signal is given by Equation (3.22). The error consists of the difference between the desired modal state, $a_{rnd}(t)$,and the actual modal state $a_{rn}(t)$. The modal state is calculated using what [Ray, 1981] calls the *modal analyzer* given by Equation (3.23):

$$a_{rn}(t) = \int_0^1 \rho(z)x_r(z,t)\phi_{rn}(z)dz \tag{3.22}$$

$$e_n = a_{rnd}(t) - a_{rn}(t) \tag{3.23}$$

where $a_{rnd}(t)$ is the desired setpoint trajectory in the modal space calculated using Equation (3.22). The setpoint trajectory was chosen to be a steady state operating profile (see Section 3.31). In practice, however, the choice of the setpoint trajectory is not trivial. Ideally, the setpoint trajectory would be chosen based on some 'optimal operating profile' in the reactor. The determination of optimal operating profiles has been the subject of recent research; one may consult Smets et al. [2001] for more detail.

The control action is calculated in this modal space and is converted back to its real state (in this case the control variable is $x_{r,in}(t)$) using Equation (3.8). This procedure is depicted in the flowsheet of Figure 3.5.

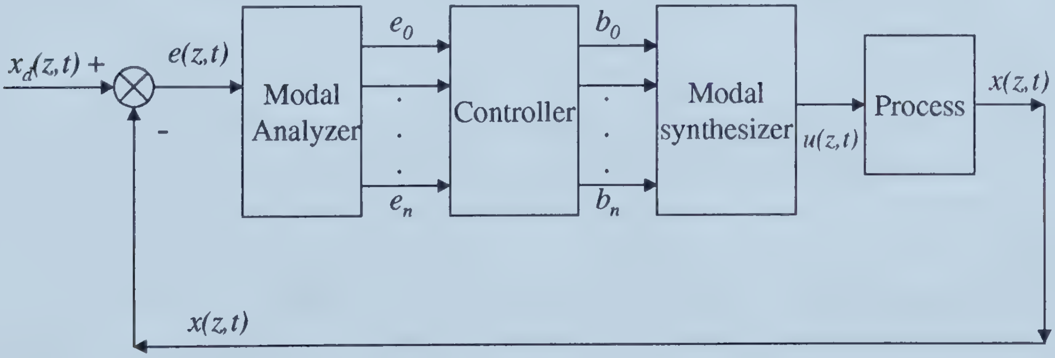

Figure 3.5: A Distributed Parameter Modal Control Scheme (taken from [Ray, 1981]).

The calculation of the control action is in essence an optimization problem, as the typical MPC problem contains an over-determined set of equations (due to the fact that in general m is chosen to be smaller than p). In this case, the unconstrained[4] problem was solved. This

---

[4] No contraints were put on the manipulated or output variables.

is essentially the same as solving a classical least squares problem which has an analytical solution.

In principle, this control scheme requires that the complete state $x(z,t)$ be available as an output. In reality, however, this is usually not possible. It is possible, however, to get this information in a few ways. Ray [1981] suggests two viable alternatives for obtaining the state information $x(z,t)$:

- One can measure $x(z_i,t),\ i = 1,2,3...l$ at a large number of points and smooth the data to get $x(z,t)$.
- One can measure $x(z_i,t)$ at a few points (possibly just one) and use a state estimator to provide estimates for $x(z,t)$.

3.2.1 Simulations

A Model Predictive Controller was designed for the system given by Equation (3.12) (or Equation (3.20) and (3.21)) in state-space form using five modes. The simulation tested a change in setpoint from an initial profile of zero across the reactor to a profile given by the steady state shown in Figure 3.4[5]. Using Equation (3.22), the desired states were calculated to be

$$a_{nd} = [0.3985, 0.1022, 0.0325, 0.0152, 0.0087]$$

A prediction horizon of five ($p = 5$)[6] and a control horizon of one ($m = 1$) were used. A control horizon greater than one resulted in aggressive control action and oscillations. One can see from Figure 3.6 that the outputs reach their setpoint values quickly ($t < 20s$). One can also observe that the steady state manipulated variable u, or in this case $x_{r,in}$ is in fact equal to one. This confirms that we have produced the desired output, since the setpoint profiles was generated using an input concentration of $x_{r,in} = 1$.

The complete concentration profile is shown in Figure 3.7. One can see the downward sloping profile at steady state is achieved. The integral of the square error between the setpoint profile and the actual output was calculated to be 0.0025 and plots of the setpoint and output profiles at steady state are shown in Appendix C. The error is not due to poor control, it is simply due to the fact that the model was approximated by only five modes. In comparison, the square error between the setpoint profile and the actual output was calculated to be 0.0007675 for $n = 10$. Several other simulations were done, varying the number of modes ($n = 2...11$) to see the effect of additional modes on the output.

---

[5] The setpoint was a smooth function given by the analytical solution of the spatial ODE with an input of $x_{r,in} = 1$. $Setpoint = 0.02314e^{\frac{\overline{5+139z}}{10}} + 0.605e^{-\frac{\overline{5+139z}}{10}}$

[6] This prediction horizon was a tuning parameter, and was chosen to be $p = 5$ to balance the tradeoff between conservative control action and computational effort.

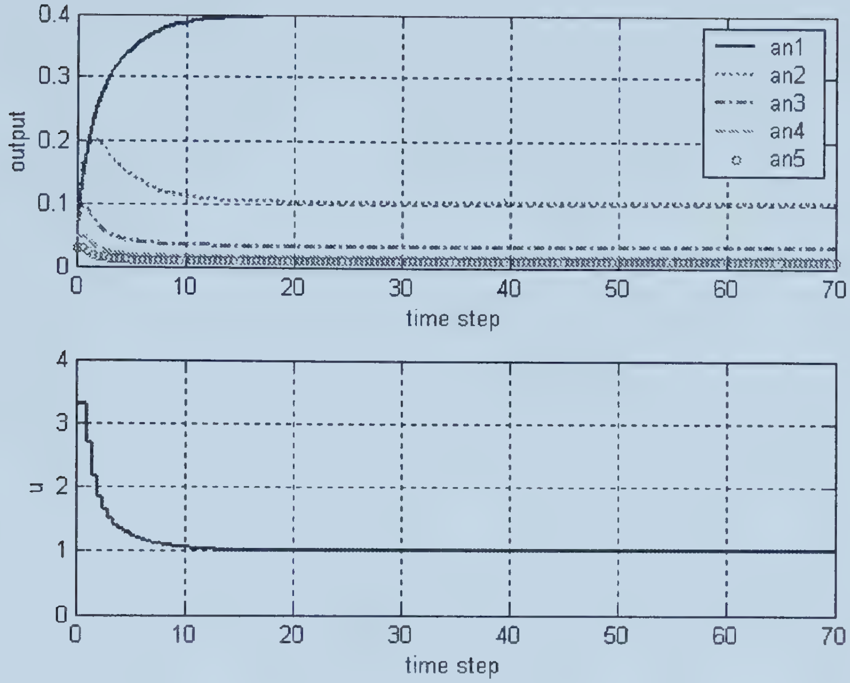

Figure 3.6: Model Predictive Control: Modal Output and Manipulated Variable Action.

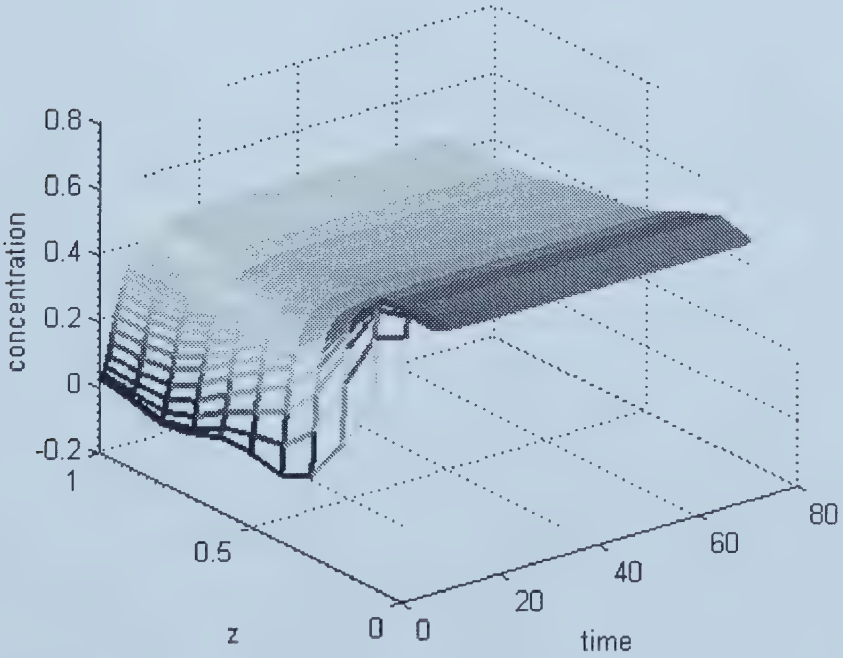

Figure 3.7: Concentration Output Using Model Predictive Control.

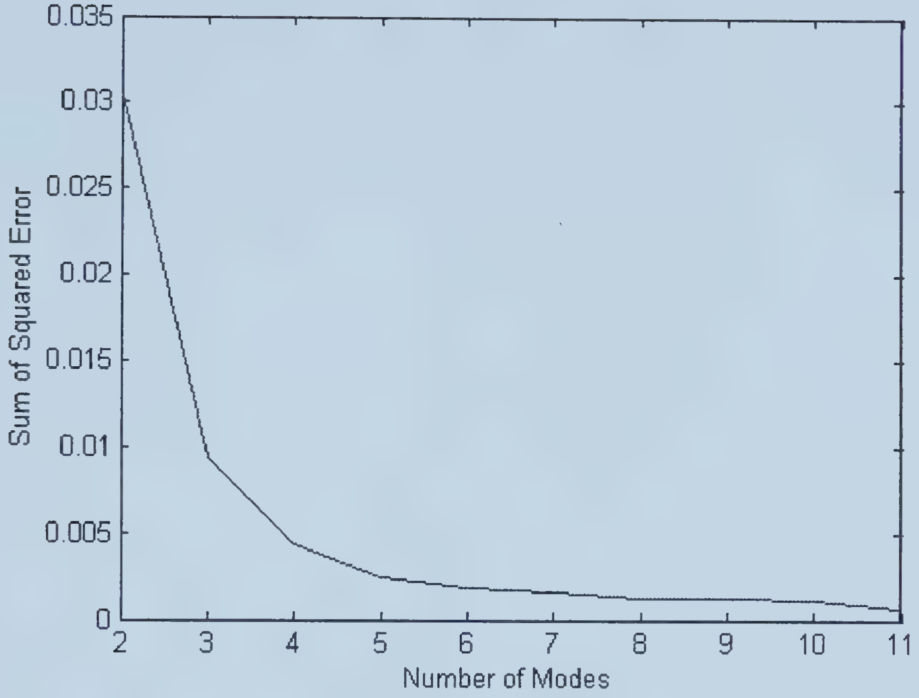

Figure 3.8: Effect of the Number of Modes on the Error Between the Setpoint and Actual Output (using MPC).

3.2.2 Discussion

Figure 3.8 shows that the error sharply decreases until five modes, where the effect of additional modes becomes less significant. This proves that there is potential for combining this lumping technique with advanced control techniques in order to reduce model order compared to their finite difference model counterpart. There is little research in the literature combining modal decomposition and advanced control techniques.

Mäder [1976] applied a modal PI controller to a parabolic heat transfer model and found that six eigenfunctions were sufficient to provide a good representation of both the state and control variables. Similar work was done by Mastumoto et al. using a PI controller on a heat transfer model. Mastumoto et al. showed that a truncation of $n = 3$ was sufficient to produce good results. They carried out comparative experiments using a finite difference model approximation, and found that similar control performance was obtained with eleven discretization points. This work was continued in [Elisante and Matsumoto, 1999*b*] where an IMC controller was implemented on the heat transfer system. To the authors knowledge, however, this research is the first to combine model predictive control with modal decomposition.

Modal decomposition has the distinct advantage of using the spectral information of the spatial differential operator instead of simply discretizing in space. With the advent of

faster computers, and hence decrease in computational times, there seemed to be a decrease in interest in modal techniques, as finite difference methods became easier to implement. It is important to note, however, that modal decomposition does in fact result in systems of lower dimension, which when combined with control techniques result in less *on-line* computation. It will be shown in chapter 4, that modal decomposition with just five modes provides a good approximation to the original system in comparison to a finite difference model with 200 equally spaced mesh points. If a controller were to be designed in this modal space, the matrix inversions involved in the computation of control action would be less computationally demanding. With the modal model, the models would include 5 by 5 matrices; whereas with the finite difference model, they would include 200 by 200 matrices. So, although a fairly large amount of analysis is required to produce the modal model, the computation is done *off-line*, and as a result the on-line computation time is significantly reduced. This should translate to a savings in computational demand (e.g., hardware requirements) for the control engineer.

The principal disadvantage of conventional modal decomposition, is that it may only be applied to linear systems. Chapter 3, showed promising results (for the linear case) for the combination of modal decomposition and model predictive control for significantly reducing model order and therefore on-line computational time. Unfortunately many processes in chemical engineering are inherently nonlinear. More specifically, it is more common for the reaction rates of convection-reaction-diffusion systems to be of greater order than 1; creating nonlinear terms. It is therefore the objective of the next chapter to undertake a preliminary investigation of modal decomposition to a nonlinear system by applying the lumping technique to a nonlinear model that has been linearized around an operating trajectory.

Chapter 4

Modal Decomposition of a Bleaching Reactor Model

Modal decomposition was discussed in Chapter 3 for a linear convection-diffusion-reaction system. The goal of this chapter is to apply modal decomposition to an industrial application (pulp bleaching) and to evaluate this method for the potential use in future control applications. A framework is established for producing the linear tangent model and performing the modal decomposition to convert the nonlinear DPS to a control-relevant form.

Bleaching wood pulp is one of the last steps in pulp processing. Environmental concerns and pressure to increase production rates have created changes in the chemical processes used in bleaching, the amounts of chemicals used, and the conditions under which the reactions take place. Bleaching costs include the costs of the chemicals as well as other costs such as steam and energy [Dence and Reeve, 1996]. An effective tool for lowering these costs is to control the process more efficiently. It is therefore important that the process be modelled in control relevant forms, which permit easier implementation of effective control strategies. This creates a challenge for a control or process engineer to understand the dynamics of the process so that control strategies can be effectively applied. Bleaching reactors can be modeled as convection-diffusion-reaction systems, which are DPS amenable to modal decomposition. The DPS is decomposed into a lumped parameter system, at which time conventional control techniques can be applied. This method also prevents the loss of spectral information that other techniques (such as finite difference methods) do not capture.

The first section of this chapter describes the bleaching process in more detail. Following this, the distributed parameter model for a bleaching reactor is presented. Modal decomposition is then extended to this nonlinear model.

The major challenges encountered in this case study are two fold: first, the bleaching reactor model consists of a coupled set of nonlinear PDEs. The PDEs were first linearized by using a first-order Taylor approximation of the bilinear reactions terms. Deviation variables were then introduced, which required the calculation of the steady state concentration profiles. The resulting set of steady state ODEs were nonlinear and didn't appear to have

an analytical solution; they were therefore solved numerically. Numerical solution of these ODEs was followed by a step whereby functions were fitted to the steady state solutions. Modal decomposition of this linearized PDE model involved the solution of the spatial ODE which involves four variable changes in order to obtain and ODE which has an analytical solution yielding the eigenfunctions. The resulting eigenfunctions of the spatial operator are Modified Bessel Functions of complex order, which are not common in the literature. A number of simulations as well as a comparative study with finite difference results was performed.

4.1 Chemical Bleaching Process

The principle objective of pulp bleaching is to achieve a high brightness. This objective must be met without compromising the strength of the final product, which can occur if there is significant cellulose degradation during bleaching. The colour in the pulp is due for the most part to lignin: a natural polymer occurring in the pulp. In Kraft pulping (which is the method we use here), the bleaching is an extension of the fibre delignification process started in the digester. Chlorine dioxide is one of the most important chemicals used in bleaching chemical pulp because it reacts readily with lignin, yet does not react to a significant extent with the carbohydrates (cellulose) [Dence and Reeve, 1996].

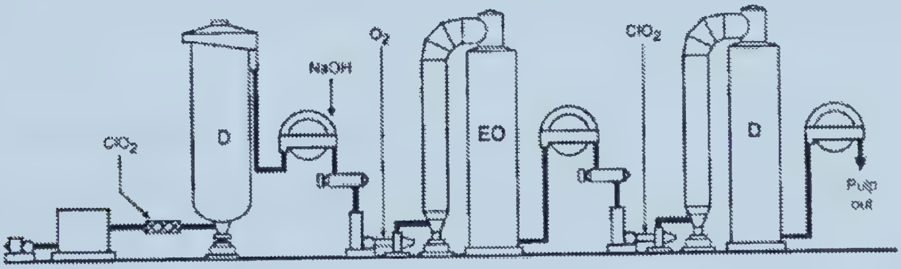

Figure 4.1: Example Flowsheet of a Bleaching Sequence (taken from [Dence and Reeve, 1996].)

Figure 4.1 shows a typical sequence of bleaching reaction and rinsing steps. The bleaching sequence designation is specified by TAPPI, where each letter is used to describe a stage of chemical application followed by washing [Dence and Reeve, 1996]. For instance, in Figure 4.1, the first tower has a designation 'D' followed then by a 'EO' tower and then a 'D' tower. This sequence, D(EO)D, refers to a chlorine dioxide treatment (D) followed by a sodium hydroxide addition, oxygen addition and washing (EO), followed by another chlorine dioxide and washing step (D).

For the purpose of this thesis, only one chlorine dioxide bleaching tower will be consid-

ered. The model that will be used was developed by [Renou, 2000] (the kinetics data was obtained from [Savoie and Tessier, 1997]). One may refer to [Renou, 2000] for more detail.

4.2 Bleaching Reactor Model

The bleaching reactor model is more complicated than the example shown in Chapter 3 and, as a result, several steps must be taken in order make the model amenable to modal decomposition. First, the bleaching reactor consists of a set of nonlinear coupled PDEs. This creates a problem, since modal decomposition is only possible on linear systems [Ray, 1981]. The model must therefore first be linearized around a chosen operating trajectory. Linearizing around a steady state operating point first requires the determination of the steady state concentration profile in the reactor. This is found by solving the set of nonlinear steady state ODEs. Unfortunately, there is no analytical solution for this particular set and the steady state profiles for lignin and chlorine were found by numerical integration of the nonlinear ODEs. Numerical integration[1], results in concentrations at discrete spatial and temporal points along the reactor representing the steady state profiles; whereas, we require a function in order to proceed with modal decomposition of the linearized model. The numerical integration data may then be fit with an appropriate function (exponential). This lead to an explicit function of the spatial variable, 'z' appearing in the set of PDEs. Nevertheless, one may proceed with the modal decomposition of the linearized model. The modal decomposition in itself requires several steps, which will be discussed in detail in the later sections. A brief list of the steps required to prepare the model for modal decomposition includes:

1. linearization of nonlinear PDE model
2. numerical solution of steady state
3. exponential fit to numerical solution
4. modal decomposition of tangent linear model.

The following subsections will be dedicated to showing each of these steps in more detail.

4.2.1 Nonlinear Model and Linear Tangent Model

The bleaching reactor model consists of a set of nonlinear coupled PDEs. The two reactants in the model are chlorine dioxide (C) and lignin (L). One can observe that Equation (4.1) is a parabolic PDE, not unlike the convection-reaction-diffusion PDE seen in Chapter 3. The main difference, however, lies in the reaction term. The reaction term is a bilinear

---

[1] One could have chosen a collocation approach using interpolating functions; however, this would have been needlessly complicated for our purposes.

term. The model must therefore first be linearized around an operating point. The PDEs describing the reactor dynamics are[2]:

$$\begin{aligned}\frac{\partial L}{\partial t} &= -v\frac{\partial L}{\partial z} + D\frac{\partial^2 L}{\partial z^2} - k_l LC \\ \frac{\partial C}{\partial t} &= -v\frac{\partial C}{\partial z} + D\frac{\partial^2 C}{\partial z^2} - k_c LC\end{aligned} \tag{4.1}$$

and the boundary conditions are:

$$\begin{aligned}\frac{\partial L(0,t)}{\partial z} &= \frac{v}{D}(L(0,t) - L_{in} - L_o) \\ \frac{\partial L(1,t)}{\partial z} &= 0 \\ \frac{\partial C(0,t)}{\partial z} &= \frac{v}{D}(C(0,t) - C_{in} - C_o) \\ \frac{\partial C(1,t)}{\partial z} &= 0\end{aligned} \tag{4.2}$$

where C_{in} and L_{in} are the inlet chlorine and lignin concentrations, respectively; and C_o and L_o are constant adjustment parameters determined from the kinetic studies done by [Savoie and Tessier, 1997]. The linearized version of the complete bleaching reactor model can be found using the first two terms of the Taylor series expansion around steady state operating profiles L_{ss} and C_{ss}:

$$\begin{aligned}\frac{\partial L}{\partial t} &\approx -v\frac{\partial L}{\partial z} + D\frac{\partial^2 L}{\partial z^2} - [k_l L_{ss}(C - C_{ss}) + k_l C_{ss}(L - L_{ss}) + k_l C_{ss} L_{ss}] \\ \frac{\partial C}{\partial t} &\approx -v\frac{\partial C}{\partial z} + D\frac{\partial^2 C}{\partial z^2} - [k_c L_{ss}(C - C_{ss}) + k_c C_{ss}(L - L_{ss}) + k_c C_{ss} L_{ss}]\end{aligned} \tag{4.3}$$

where L_{ss} and C_{ss} are the steady state lignin and chlorine profiles. The steady state equations are given by:

$$\begin{aligned}\frac{\partial L_{ss}}{\partial t} &= 0 = -v\frac{\partial L_{ss}}{\partial z} + D\frac{\partial^2 L_{ss}}{\partial z^2} - k_l L_{ss} C_{ss} \\ \frac{\partial C_{ss}}{\partial t} &= 0 = -v\frac{\partial C_{ss}}{\partial z} + D\frac{\partial^2 C_{ss}}{\partial z^2} - k_c L_{ss} C_{ss}\end{aligned} \tag{4.4}$$

with steady state boundary conditions given by:

$$\begin{aligned}\frac{\partial L_{ss}(0)}{\partial z} &= \frac{v}{D}(L_{ss}(0) - L_{in,ss} - L_o) \\ \frac{\partial L_{ss}(1)}{\partial z} &= 0 \\ \frac{\partial C_{ss}(0)}{\partial z} &= \frac{v}{D}(C_{ss}(0) - C_{in,ss} - C_o) \\ \frac{\partial C_{ss}(1)}{\partial z} &= 0\end{aligned} \tag{4.5}$$

---

[2] The reader should note that the procedure for modal decomposition remains the same reagardless of the order of the reaction kinetics. These bilinear kinetics are the simplest of the nonlinear kinetic models. However, once linearized, the resulting model takes the same form, regardless of the order of the nonlinear reaction kinetics (e.g., $(LC)^2$ or $(LC)^3$)

Subtracting Equation (4.4) from Equation (4.3), and letting $\widetilde{C} = C - C_{ss}$ and $\widetilde{L} = L - L_{ss}$, one obtains:

$$\begin{aligned} \frac{\partial \widetilde{L}}{\partial t} &= -v\frac{\partial \widetilde{L}}{\partial z} + D\frac{\partial^2 \widetilde{L}}{\partial z^2} - k_l L_{ss}\widetilde{C} - k_l C_{ss}\widetilde{L} \\ \frac{\partial \widetilde{C}}{\partial t} &= -v\frac{\partial \widetilde{C}}{\partial z} + D\frac{\partial^2 \widetilde{C}}{\partial z^2} - k_c L_{ss}\widetilde{C} - k_c C_{ss}\widetilde{L} \end{aligned} \tag{4.6}$$

$$\begin{aligned} \frac{\partial \widetilde{L}(0,t)}{\partial z} &= \frac{v}{D}(\widetilde{L}(0,t) - \widetilde{L}_{in}) \\ \frac{\partial L(1,t)}{\partial z} &= 0 \\ \frac{\partial C(0,t)}{\partial z} &= \frac{v}{D}(\widetilde{C}(0,t) - \widetilde{C}_{in}) \\ \frac{\partial C(1,t)}{\partial z} &= 0 \end{aligned} \tag{4.7}$$

The original nonlinear PDE set has now been linearized around steady state operating conditions. One must now determine the chlorine and lignin profiles (C_{ss} and L_{ss}) associated with this steady state.

4.2.2 Numerical Solution of Steady State Profiles

To find the steady state concentration profiles, one must solve the following nonlinear coupled system of ODEs:

$$\begin{aligned} -v\frac{dL_{ss}}{dz} + D\frac{d^2 L_{ss}}{dz^2} - k_l L_{ss} C_{ss} &= 0 \\ -v\frac{dC_{ss}}{dz} + D\frac{d^2 C_{ss}}{dz^2} - k_c C_{ss} L_{ss} &= 0 \end{aligned} \tag{4.8}$$

$$\begin{aligned} \frac{dC_{ss}(0)}{dz} &= \frac{v}{D}\left(C_{ss}(0) - C_{in,ss} - C_o\right) \\ \frac{dC_{ss}(1)}{dz} &= 0 \\ \frac{dL_{ss}(0)}{dz} &= \frac{v}{D}\left(L_{ss}(0) - L_{in,ss} - L_o\right) \\ \frac{dL_{ss}(1)}{dz} &= 0 \end{aligned} \tag{4.9}$$

In order to simplify their solution, we perform a change of variable (that triangularizes[3] the system). Let:

$$\xi_1 = k_c L_{ss} - k_l C_{ss} \tag{4.10}$$

---

[3] In other words, this decouples the PDE set in such a way that the first PDE no longer depends on the second; and only the second PDE depends on the first.

and therefore:

$$\begin{aligned} \xi_1(0) &= k_c L_{ss}(0) - k_l C_{ss}(0) \\ \xi_{1in} &= k_c(L_{in,ss} - Lo) - k_l(C_{in,ss} - Co) \end{aligned} \tag{4.11}$$

The resulting ODE set in the new variable with its boundary conditions is:

$$\begin{aligned} -v\frac{d\xi_1}{dz} + D\frac{d^2\xi_1}{dz^2} &= 0 \\ \frac{d\xi_1(0)}{dz} &= \frac{v}{D}\left(\xi_1(0) - \xi_{1in}\right) \\ \frac{d\xi_1(1)}{dz} &= 0 \end{aligned} \tag{4.12}$$

The solution to this ODE set is:

$$\xi_1 = \xi_{1in} \tag{4.13}$$

Creating a new variable $\xi_2 = C_{ss}$, we can write down the steady state ODE:

$$-v\frac{d\xi_2}{dz} + D\frac{d^2\xi_2}{dz^2} - k_c L_{ss}\xi_2 = 0 \tag{4.14}$$

and substituting the expression $k_c L_{ss} = \xi_1 + k_l C_{ss}$ (from Equation (4.24)) yields:

$$-v\frac{d\xi_2}{dz} + D\frac{d^2\xi_2}{dz^2} - \left(\xi_1 + k_l\xi_2\right)\xi_2 = 0 \tag{4.15}$$

or expanding:

$$-v\frac{d\xi_2}{dz} + D\frac{d^2\xi_2}{dz^2} - \xi_1\xi_2 - k_l\xi_2^2 = 0 \tag{4.16}$$

$$\begin{aligned} \frac{d\xi_2(0)}{dz} &= \frac{v}{D}\left(\xi_2(0) - \xi_{2in}\right) \\ \frac{d\xi_2(1)}{dz} &= 0 \end{aligned} \tag{4.17}$$

Substituting Equation (4.13) yields the nonlinear ODE shown below:

$$-v\frac{d\xi_2}{dz} + D\frac{d^2\xi_2}{dz^2} - \xi_{1in}\xi_2 - k_l\xi_2^2 = 0 \tag{4.18}$$

$$\begin{aligned} \frac{d\xi_2(0)}{dz} &= \frac{v}{D}\left(\xi_2(0) - \xi_{2in}\right) \\ \frac{d\xi_2(1)}{dz} &= 0 \end{aligned} \tag{4.19}$$

The ODE set given by Equation (4.18) is a fairly simple ODE yet still nonlinear. The reasoning behind the change of variable is that it is easier to find an analytical solution to a

single ODE than for a coupled ODE set (or at least it is easier to see whether an analytical solution exists). Despite this, it does not appear to have an analytical solution. It must therefore be solved numerically. To simplify for programming purposes, we perform another change of variable:

$$\begin{aligned} \beta_1 &= \xi_2 \\ \beta_2 &= \frac{d\xi_2}{dz} \end{aligned} \tag{4.20}$$

This reduces the second order ODE to a system of two first ODEs:

$$\begin{aligned} \frac{d\beta_1}{dz} &= \beta_2 \\ \frac{d\beta_2}{dz} &= \frac{1}{D}\left[v\beta_2 + k_l\beta_1^2 + \xi_{1in}\beta_1\right] \end{aligned} \tag{4.21}$$

This new system in β must have "artificial" boundary conditions created. This is because it is numerically easier to solve ODEs with only initial conditions, than ODEs with both initial and final conditions. The boundary conditions are therefore:

$$\begin{aligned} \beta_1(0) &= \xi_2(0) \\ \beta_2(0) &= \frac{v}{D}(\xi_2(0) - \xi_{2in}) \end{aligned} \tag{4.22}$$

The problem lies in the fact that $\xi_2(0)$ is unknown. Therefore we proceed by an iterative procedure whereby $\xi_2(0)$ is given a value and it is verified that the profile near the end of the reactor is flat in order to satisfy the "zero flux" boundary condition in ξ_2 at the exit of the reactor given by Equation (4.19). Table 4.1 lists the steady state operating conditions for the solution of C_{ss} and L_{ss}.

Table 4.1: Steady State Operating Parameters

k_c	0.006
k_l	0.035
Lin_{ss}	31 Kappa
Lo	9 Kappa
Cin_{ss}	2.5 g/l
Co	1.3 g/l
v	1/30 min
D	0.5/30

Results of the numerical integration are shown in Figure 4.2 below.

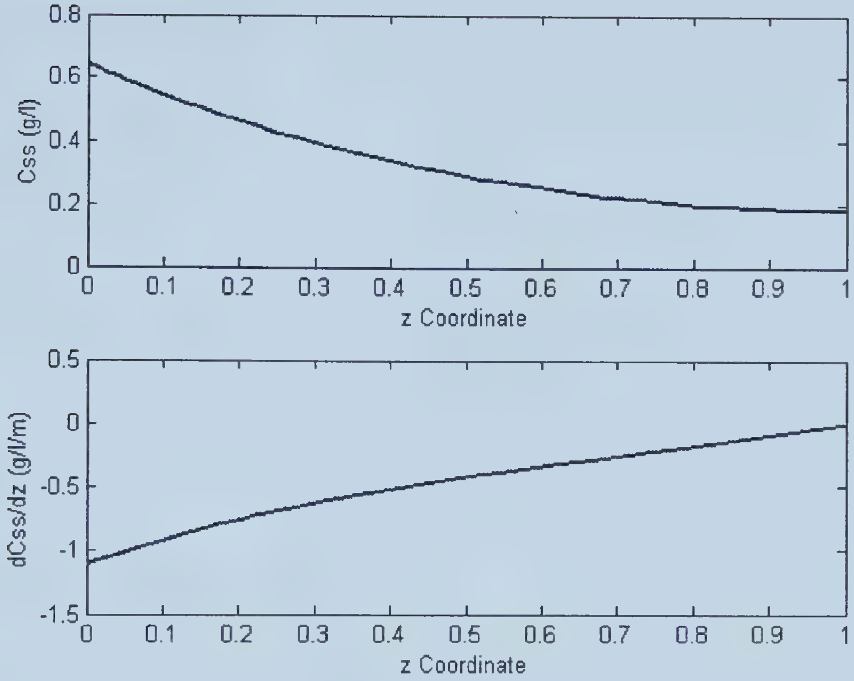

Figure 4.2: Numerical Integration Results - C_{ss} and its Derivative.

An exponential model was then fitted to the results of the numerical integration. Figure 4.3 shows the results of the integration. A least squares fit was done on the log of the data, and the sum of the squared errors was 0.0066. Other trial functions (e.g., polynomials of various orders) were tested to see if they resulted in better fit, however the exponential function provided the best fit. Also, as will be shown later in the chapter, the benefit of having chosen a simple exponential function to fit C_{ss} and L_{ss}, is that as a consequence, there exists an analytical solution of the spatial ODE.

The resulting exponential models for both C_{ss} and L_{ss} are:

$$\begin{aligned} C_{ss} &= 0.6459e^{-1.5675z} \\ L_{ss} &= \frac{\xi_{in} + k_l C_{ss}}{k_c} = 15 + 3.7678e^{-1.5675z} \end{aligned} \tag{4.23}$$

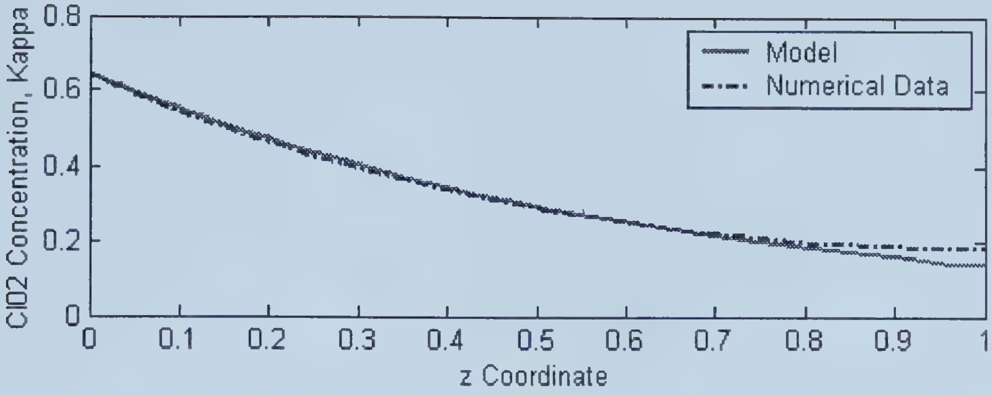

Figure 4.3: Exponential Model Fit to C_{ss} Data Obtained by Numerical Integration.

4.3 Modal Decomposition

This section is dedicated to the modal decomposition of the linearized bleaching reactor model (given by Equation (4.6) and Equation (4.7) and restated below for convenience). The procedure is divided up into several sections, as the solution procedure is quite involved.

The first section triangularizes the system to yield one independent PDE and a second PDE with a cross term in the other variable. The first PDE is easily decomposed with the methods shown in Chapter 2. The second PDE requires the use of eigenfunction expansion and several variable changes before yielding a solution with Modified Bessel functions of complex order.

$$\begin{aligned}
\frac{\partial \widetilde{L}}{\partial t} &= -v\frac{\partial \widetilde{L}}{\partial z} + D\frac{\partial^2 \widetilde{L}}{\partial z^2} - k_l L_{ss}\widetilde{C} - k_l C_{ss}\widetilde{L} \\
\frac{\partial \widetilde{C}}{\partial t} &= -v\frac{\partial \widetilde{C}}{\partial z} + D\frac{\partial^2 \widetilde{C}}{\partial z^2} - k_c L_{ss}\widetilde{C} - k_c C_{ss}\widetilde{L}
\end{aligned}$$

$$\begin{aligned}
\frac{\partial \widetilde{L}(0,t)}{\partial z} &= \frac{v}{D}(\widetilde{L}(0,t) - \widetilde{L}_{in}) \\
\frac{\partial \widetilde{L}(1,t)}{\partial z} &= 0 \\
\frac{\partial \widetilde{C}(0,t)}{\partial z} &= \frac{v}{D}(\widetilde{C}(0,t) - \widetilde{C}_{in}) \\
\frac{\partial \widetilde{C}(1,t)}{\partial z} &= 0
\end{aligned}$$

4.3.1 Triangularized System

In order to decompose the linearized bleaching reactor model Equation (4.6) into its modes, we first triangularize the system using a similar transformation to that given in Equation

(4.10):

$$\eta_1 = k_c\widetilde{L} - k_l\widetilde{C} \tag{4.24}$$

and

$$\eta_2 = \widetilde{C} \tag{4.25}$$

This change of variable yields the following set of PDEs with boundary conditions:

$$\frac{\partial \eta_1}{\partial t} = -v\frac{\partial \eta_1}{\partial z} + D\frac{\partial^2 \eta_1}{\partial z^2} \tag{4.26}$$

$$\frac{\partial \eta_2}{\partial t} = -v\frac{\partial \eta_2}{\partial z} + D\frac{\partial^2 \eta_2}{\partial z^2} - k_c L_{ss}\eta_2 - C_{ss}\left(\eta_1 + k_l\eta_2\right) \tag{4.27}$$

$$\begin{aligned} \frac{\partial \eta_1(0,t)}{\partial z} &= \frac{v}{D}(\eta_1(0,t) - \eta_{1in}) \\ \frac{\partial \eta_1(1,t)}{\partial z} &= 0 \end{aligned} \tag{4.28}$$

$$\begin{aligned} \frac{\partial \eta_2(0,t)}{\partial z} &= \frac{v}{D}(\eta_2(0,t) - \eta_{2in}) \\ \frac{\partial \eta_2(1,t)}{\partial z} &= 0 \end{aligned} \tag{4.29}$$

This transformation eliminated the reaction term from the first PDE given in Equation (4.6); and is related to the notion of reaction invariants [Gavalas, 1968; Bastin and Dochain, 1990]. The physical significance of η_1 is that it represents the difference between the amounts of chlorine and lignin reacting, and since these two chemicals react according to the stoichiometry of the reaction, at steady state it was shown that this value is merely a constant ($\xi_1 = \xi_{1in}$ by Equation (4.13)). Also, η_2 simply represents the concentration of lignin as shown by Equation (4.25).

The decomposition of Equation (4.26) is essentially identical to the decomposition shown in Chapter 3 (i.e., the eigenvalues and eigenfunctions are identical to Equations (3.13) through (3.15) with $k = 0$). The second PDE, given by Equation (4.27) is more complicated, as the exponential functions from the steady state solutions appear as explicit functions of z for the coefficients. The next subsection will deal with the decomposition of Equation (4.26). Following this, Equation (4.27) will be treated.

4.3.2 Decomposition of First PDE

As in Chapters 2 and 3, the first PDE is linear with linear boundary conditions, therefore we may proceed as before. Substituting the following expressions:

$$\eta_1(z,t) = \sum_{n=1}^{\infty} p_{\psi n}(t)\psi_n(z) \tag{4.30}$$

$$\delta(z)\eta_{1in}(t) = \sum_{n=0}^{\infty} q_n(t)\,\psi_n(z) \tag{4.31}$$

into Equation (4.26) yields a set of separable ODEs in time and space:

$$\frac{dp_{\psi n}(t)}{dt} + \lambda_\psi p_{\psi n}(t) = q_n(t) \tag{4.32}$$

$$\begin{aligned} D\frac{d^2\psi_n}{dz^2} - v\frac{d\psi_n}{dz} + \lambda_\psi\psi_n &= 0 && (4.33)\\ v\frac{d\psi_n(0)}{dz} + D\psi(0) &= 0 && (4.34)\\ \frac{d\psi_n(1)}{dz} &= 0 && (4.35) \end{aligned}$$

The solution to Equation (4.33) (using separation of variables) is:

$$\psi_n(z) = G_n e^{\frac{v}{2D}z}\left[\cos\left(\frac{s_{\psi n}}{2D}z\right) + \frac{v}{s_n}e^{\frac{v}{2D}z}\sin\left(\frac{s_{\psi n}}{2D}z\right)\right] \tag{4.36}$$

where:

$$s_{\psi n} = \sqrt{v^2 - 4D\lambda_{\psi n}} \tag{4.37}$$

On application of the boundary conditions, $s_{\psi n}$, are found by solving Equation (3.14):

$$\tan\left(\frac{L}{2D}s_{\psi n}\right) = \frac{2vs_{\psi n}}{s_{\psi n}^2 - v^2} \tag{4.38}$$

Therefore the eigenvalues, $\lambda_{\psi n}$, can be found by rearranging Equation (4.37):

$$\lambda_{\psi n} = -\frac{s_{\psi n}^2 + v^2}{4D} \tag{4.39}$$

Using the properties of orthogonal functions and Sturm-Liouville theory, the G_n coefficients are chosen such that $\|\psi_n\|_2 = 1$. With the eigenvalues, $\lambda_{\psi n}$, one may then solve Equation (4.32).

4.3.3 Simulation

The conditions under which the simulation of $\eta_1(z,t)$ was done were the following:

- At $t = 0$, initial conditions were such that the reactor had a profile other than that of steady state ($\eta_1(z,0) = 0.1$).
- It was assumed that there was no variation from the steady-state value of the input ($\eta_{1in}(t) = 0$)

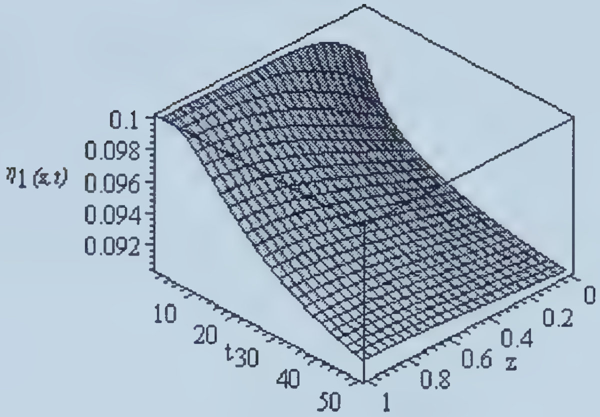

Figure 4.4: Unforced Solution of $\eta_1(z,t)$.

The solution is then given by:

$$\eta_1(z,t) = \sum_{n=1}^{\infty} \left[e^{\lambda_{\psi n} t} \left\langle \eta_{1,0}, \widetilde{\psi_n} \right\rangle \psi_n \right] \tag{4.40}$$

Where $\widetilde{\psi_n}$ are the eigenfunctions of the adjoint operator (where M_n are chosen such that $\left\|\widetilde{\psi_n}\right\|_2 = 1$:

$$\widetilde{\psi_n} = M_n \psi_n(L - z) \tag{4.41}$$

. The solution with the first five terms in the series is:

$$\eta_1(z,t) = e^z \left[\begin{array}{c} 0.005359e^{-.0451t}(\cos(1.307z) + .7654\sin(1.307z)) \\ +0.002258e^{-.2415t}(\cos(3.673z) + .2722\sin(3.673z)) \\ +.0008434e^{-.7393t}(\cos(6.585z) + .1519\sin(6.585z)) \\ +.0004132e^{-1.562t}(\cos(9.632z) + .1038\sin(9.632z)) \\ +.000241e^{-2.714t}(\cos(12.723z) + .0786\sin(12.723z)) \end{array} \right] \tag{4.42}$$

Figure 4.4 depicts $\eta_1(z,t)$ from its initial state of 0.1 to the steady state of 0.09.

With the full solution of $\eta_1(z,t)$, we can now proceed with the solution of the second PDE in $\eta_2(z,t)$.

4.3.4 Decomposition using Eigenfunction Expansion - Second PDE:

The modal decomposition of Equation (4.27) is more complicated, due to the exponential terms in 'z', and the presence of a term in η_1. This PDE is not amenable to the separation of variables method; however, the technique of eigenfunction expansion may be used (Street, 1973):

$$\frac{\partial \eta_2}{\partial t} = -v\frac{\partial \eta_2}{\partial z} + D\frac{\partial^2 \eta_2}{\partial z^2} - k_c L_{ss}\eta_2 - C_{ss}\left(\eta_1 + k_l\eta_2\right)$$

Substituting Equation (4.23):

$$\frac{\partial \eta_2}{\partial t} = -v\frac{\partial \eta_2}{\partial z} + D\frac{\partial^2 \eta_2}{\partial z^2} - k_c(15 + 3.7678e^{-1.5675z})\eta_2 - \left(0.6459e^{-1.5675z}\right)\left(\eta_1 + k_l\eta_2\right) \tag{4.43}$$

and combining terms yields:

$$\frac{\partial \eta_2}{\partial t} = -v\frac{\partial \eta_2}{\partial z} + D\frac{\partial^2 \eta_2}{\partial z^2} - (0.09 + 0.04521e^{-1.5675z})\eta_2 - \left(0.6459e^{-1.5675z}\right)\left(\eta_1\right) \tag{4.44}$$

If the term in $\eta_1 = 0$, then Equation (4.27) may be decomposed using the separation of variables method shown above (and in Chapter 2). In that case, after separation of variables, an eigenvalue problem is formulated and can be solved. The eigenfunctions, together with appropriate time-dependent functions and some free constants, can then be combined in an infinite series [Street, 1973]. Since $\eta_1(z,t) \neq 0$, one must solve the *associated* eigenvalue problem (with $\eta_1 = 0$), with η_1 regarded as an input. It will later reappear in the determination of the time varying coefficients of the infinite series expansion. To decompose Equation (4.27) into a set of ODEs, we first consider the *associated* PDE with the term in η_1 removed. As before, we let:

$$\eta_2(z,t) = \sum_{n=0}^{\infty} r_n(t)\gamma_{1n}(z) \tag{4.45}$$

We obtain ODEs in the spatial and time variables:

$$-v\frac{d\gamma_{1n}}{dz} + D\frac{d^2\gamma_{1n}}{\partial z^2} + \left[\lambda_\gamma - 0.09 - 0.04521e^{-1.5675z}\right]\gamma_{1n} = 0 \tag{4.46}$$

$$\begin{aligned} D\frac{d\gamma_{1n}(0)}{dz} - v\gamma_{1n}(0) &= 0 \\ \frac{d\gamma_{1n}(1)}{dz} &= 0 \end{aligned} \tag{4.47}$$

$$\frac{dr_n}{dt} + \lambda_\gamma r_n = 0 \tag{4.48}$$

$$r_n(0) = r_{n,0} \tag{4.49}$$

The next subsection will be dedicated to solving Equation (4.46), since it involves several change of variables.

4.3.5 Solution of Spatial ODE

The solution proposed here is based on a sequence of four successive change of variables. Equation (4.46) may be found in [Murphy, 1960] (Entry #106 in Tables of Equations of Second Order, p.321). Murphy then suggests a change of variable:

$$\begin{aligned} \gamma_{1n}(z) &= \varpi_1 \gamma_{2n}(\varpi_2) \\ \varpi_1 &= e^{-a_2 z/2} \end{aligned} \tag{4.50}$$

Substituting this change of variable into Equation (4.46) yields an ODE in the new variable:

$$\frac{d^2\gamma_{2n}(\varpi_2)}{\partial \varpi_2^2} + (b_2 - \frac{a_2^2}{4} + c_2 e^{d_2 \varpi_2})\gamma_{2n}(\varpi_2) = 0 \tag{4.51}$$

with:

$$\begin{aligned} a_2 = &\quad -\tfrac{v}{D} \\ b_2 = &\quad \tfrac{(\lambda_\gamma - 0.09)}{D} \\ c_2 = &\quad -\tfrac{(0.04521)}{D} \\ d_2 = &\quad -1.5675 \\ \varpi_2 = &\quad z \end{aligned} \tag{4.52}$$

Equation (4.51) is similar to Entry #54 in Tables of Equations of Second Order [Murphy, 1960, p. 317]. Murphy then suggests a second change of variable:

$$\begin{aligned} \gamma_{2n}(\varpi_2) &= e^{-\frac{\varpi_2}{2}} \gamma_{3n}(\varpi_3) \\ \varpi_3 &= e^{\varpi_2} \end{aligned} \tag{4.53}$$

This yields a new ODE in $\gamma_{3n}(\varpi_3)$:

$$\varpi_3^2 \frac{d^2\gamma_{3n}(\varpi_3)}{d\varpi_3^2} + \left(\frac{1}{4} + a_3 + c_3 (\varpi_3)^{d_3}\right) \gamma_{3n}(\varpi_3) \tag{4.54}$$

$$\begin{aligned} a_3 = &\quad \left(b_2 - \tfrac{a_2^2}{4}\right) \\ c_3 = &\quad c_2 \\ d_3 = &\quad d_2 \end{aligned} \tag{4.55}$$

Equation (4.54) is similar to Entry #251 in Tables of Equations of Second Order [Murphy, 1960, p. 336]. Performing the following third change of variable:

$$\gamma_{3n}(\varpi_3) = (\varpi_4)^{\zeta_4} \gamma_{4n}(\varpi_4) \tag{4.56}$$

This yields a new ODE in $\gamma_{4n}(\varpi_4)$:

$$\varpi_4 \frac{d^2\gamma_{4n}(\varpi_4)}{d\varpi_4^2} + 2\zeta_4 \frac{d\gamma_{4n}(\varpi_4)}{d\varpi_4} + c_4 \left(\varpi_4\right)^{d_4-1} \gamma_{4n}(\varpi_4) \tag{4.57}$$

where:

$$\begin{aligned} \varpi_4 = {} & \varpi_3 \\ \zeta_4^2 - \zeta_4 + a_4 = {} & 0 \\ a_4 = {} & \left(\tfrac{1}{4} + a_3\right) \\ c_4 = {} & c_3 \\ d_4 = {} & d_3 \end{aligned} \tag{4.58}$$

Equation (4.57) resembles Entry #202 in Tables of Equations of Second Order [Murphy, 1960,p. 329]. Murphy then suggests fourth and final change of variable:

$$\gamma_{4n}(\varpi_4) = (\varpi_4)^{\zeta_5} \gamma_{5n}(\varpi_5) \tag{4.59}$$

This yields an ODE of the form:

$$\left(\varpi_5\right)^2 \frac{d^2\gamma_{5n}(\varpi_5)}{d\varpi_5^2} + \varpi_5 \frac{d\gamma_{5n}(\varpi_5)}{d\varpi_5} + \left(\left(\varpi_5\right)^2 - p^2\right) \gamma_{5n}(\varpi_5) \tag{4.60}$$

$$\begin{aligned} \varpi_5 = {} & Y_4 \left(\varpi_4\right)^{f_4} \\ 2\zeta_5 = {} & 1 - 2\zeta_4 \\ Y_4 d_4 = {} & \pm 2\sqrt{c_4} \\ 2f_4 = {} & d_4 \\ d_4 p = {} & 1 - 2\zeta_4 \end{aligned} \tag{4.61}$$

Equation (4.60) is the well known Bessel's Equation (Entry #274 in Murphy, p.331). Due to all the changes in variables and the numerical values of the constants, it is actually Bessel's modified equation (#275 in Murphy). Using the constants as given by the original ODE and the parameters listed in Table 4.1, Equation (4.46), the analytical solution to Equation (4.46) is given by:

$$\gamma_1(z) = \left(e^{-1.5675z}\right)^{.6378} \left[C_1 I_p \left(2.1015\sqrt{e^{-1.5675z}}\right) + C_2 I_{-p} \left(2.1015\sqrt{e^{-1.5675z}}\right)\right] \tag{4.62}$$

where I_p is a *modified Bessel function* of order p and argument $\left(2.1015\sqrt{e^{-1.5675z}}\right)$. Here, the order of the modified Bessel functions is given by:

$$p = \sqrt{10.4190 - 97.6778\lambda_\gamma} \tag{4.63}$$

For some background mathematics on Bessel and Modified Bessel functions of various orders and arguments, the reader may consult Appendix D. Murphy suggests the solutions of the

modified Bessel's Equation should take on different forms depending on the nature of the order p. The general solution of the ODE is:

$$\begin{array}{ll} \gamma(z) = C_1 I_p(z) + C_2 I_{-p} & ;\, p \text{ not an integer} \\ \gamma(z) = C_1 I_p(z) + C_2 K_p & ;\, p \text{ an integer} \end{array} \tag{4.64}$$

As can be seen from the solution of Equation (4.60), given by Equation (4.62), p is not an integer, therefore the pair of linearly independent solutions to be chosen is I_p and I_{-p}.

4.3.6 Application of Boundary conditions: determination of eigenvalues

Equation (4.62) represents the general solution to the spatial ODE in γ_{1n}. We now proceed with the full solution using the boundary conditions given by Equation (4.47). Equations (4.62) and (4.47) are repeated below for convenience.

$$\gamma_1(z) = \left(e^{-1.5675z}\right)^{.6378} \left[C_1 I_p\left(2.1015\sqrt{e^{-1.5675z}}\right) + C_2 I_{-p}\left(2.1015\sqrt{e^{-1.5675z}}\right)\right]$$

$$\begin{aligned} D\frac{d\gamma_{1n}(0)}{dz} - v\gamma_{1n}(0) &= 0 \\ \frac{d\gamma_{1n}(1)}{dz} &= 0 \end{aligned}$$

Applying the first boundary condition yields C_1 as a function of C_2.

$$C_1 = C_2 \frac{-0.125 \cdot 10^{10} I_{-p}(\theta_{\gamma 1}) - .2059 \cdot 10^{10} I_{-p+1}(\theta_{\gamma 1}) + s_{\gamma n} I_{-p}(\theta_{\gamma 1})}{.2059 \cdot 10^{10} I_{p+1}(\theta_{\gamma 1}) + s_{\gamma n} I_p(\theta_{\gamma 1}) + 0.125 \cdot 10^{10} I_p(\theta_{\gamma 1})} \tag{4.65}$$

where:

$$\theta_{\gamma 1} = 2.1015$$

$$s_{\gamma n} = 0.9797 \cdot 10^9 p$$

Substituting this expression back and solving the second boundary conditions yields

$$\begin{aligned} & C_2(-0.2556 \cdot 10^{10} I_{p+1}(\theta_{\gamma 2}) I_{-p}(\theta_{\gamma 1}) - 0.4210 \cdot 10^{10} I_{p+1}(\theta_{\gamma 2}) I_{-p+1}(\theta_{\gamma 1}) + \quad (4.66) \\ & 2.0447 I_{p+1}(\theta_{\gamma 2}) s_{\gamma n} I_{-p}(\theta_{\gamma 1}) - 5.4365 s_{\gamma n} I_p(\theta_{\gamma 2}) I_{-p}(\theta_{\gamma 1}) \\ & -4.4775 s_{\gamma n} I_p(\theta_{\gamma 2}) I_{-p+1}(\theta_{\gamma 1}) + 0.2514 \cdot 10^{11} I_p(\theta_{\gamma 2}) I_{-p}(\theta_{\gamma 1}) - \\ & 0..2039 \cdot 10^{11} I_p(\theta_{\gamma 2}) I_{-p}(\theta_{\gamma 1}) \lambda_{\gamma n} + 0.4210 \cdot 10^{10} I_{-p+1}(\theta_{\gamma 2}) I_{p+1}(\theta_{\gamma 1}) + \\ & 2.0447 I_{-p+1}(\theta_{\gamma 2}) s_{\gamma n} I_p(\theta_{\gamma 1}) + 0.2556 \cdot 10^{10} I_{-p+1}(\theta_{\gamma 2}) I_p(\theta_{\gamma 1}) - \\ & 4.4775 s_{\gamma n} I_{-p}(\theta_{\gamma 2}) I_{p+1}(\theta_{\gamma 1}) - 0.2514 \cdot 10^{11} I_{-p}(\theta_{\gamma 2}) I_p(\theta_{\gamma 1}) + \\ & 0.2039 \cdot 10^{12} I_{-p}(\theta_{\gamma 2}) I_p(\theta_{\gamma 1}) \lambda_{\gamma n} - 5.4365 s_{\gamma n} I_{-p}(\theta_{\gamma 2}) I_p(\theta_{\gamma 1}) + \\ & 0.5596 \cdot 10^{10} I_p(\theta_{\gamma 2}) I_{-p+1}(\theta_{\gamma 1}) - 0.5596 \cdot 10^{10} I_{-p}(\theta_{\gamma 2}) I_{p+1}(\theta_{\gamma 1})) \\ = \; & 0 \end{aligned}$$

where:

$$\theta_{\gamma 2} = 0.9597$$

To solve Equation (4.66) we note that $C_2 \neq 0$. If $C_2 = 0$ then $C_1 = 0$ by Equation (4.65) and this represents the trivial solution. Therefore we solve Equation (4.66) with $C_2 \neq 0$. Put differently, we must find the values of $\lambda_{\gamma n}$ such that Equation (4.66) is satisfied. One important fact should be noted about the general solution given by Equation (4.62), and Equation (4.66). The eigenvalues of the solution are related to the *order* of the modified Bessel function. Solutions to conventional ODEs involving Bessel functions tend to have the eigenvalues as functions of the zeros of the Bessel functions (on application of boundary conditions). It can be seen that upon application of the boundary conditions in this case, that the zeros of the Bessel functions will be functions of their orders. Gray et al. [1939] discuss this in some detail.

One other added complication is the value of left hand side of Equation (4.66) is complex (non-real) for varying $\lambda_{\gamma n}$. This makes finding the $\lambda_{\gamma n}$'s that solve Equation (4.66) difficult, as root finding techniques for complex valued functions are not widely available. However, according to [Gray *et al.*, 1931], modified Bessel functions of the second kind $K_p(z)$, as well as the combined function $I_p(az)K_p(bz) - I_p(bz)K_p(az)$ have no real zeros unless p (the order of the Bessel function) is purely imaginary, and it can be shown that they have an infinite number of such zeros. Although Equation (4.66) is neither of the above functions, it was thought that there was a possibility that an infinite number of $\lambda_{\gamma n}$'s which satisfied the boundary condition did exist; especially since the order of the modified Bessel functions, p, in Equation (4.66) is purely complex.

In order to simplify the explanation of the next section, let us define a name for the value of Equation (4.66) at various values of $\lambda_{\gamma n}$. Let:

$$\begin{aligned}
B.C. \;=\; & (-0.2556 \cdot 10^{10} I_{p+1}(\theta_{\gamma 2}) I_{-p}(\theta_{\gamma 1}) - 0.4210 \cdot 10^{10} I_{p+1}(\theta_{\gamma 2}) I_{-p+1}(\theta_{\gamma 1}) \qquad (4.67)\\
& +2.0447 I_{p+1}(\theta_{\gamma 2})\, s_{\gamma n} I_{-p}(\theta_{\gamma 1}) - 5.4365 s_{\gamma n} I_p(\theta_{\gamma 2}) I_{-p}(\theta_{\gamma 1})\\
& -4.4775 s_{\gamma n} I_p(\theta_{\gamma 2}) I_{-p+1}(\theta_{\gamma 1}) + 0.2514 \cdot 10^{11} I_p(\theta_{\gamma 2}) I_{-p}(\theta_{\gamma 1}) -\\
& 0..2039 \cdot 10^{11} I_p(\theta_{\gamma 2}) I_{-p}(\theta_{\gamma 1}) \lambda_{\gamma n} + 0.4210 \cdot 10^{10} I_{-p+1}(\theta_{\gamma 2}) I_{p+1}(\theta_{\gamma 1}) +\\
& 2.0447 I_{-p+1}(\theta_{\gamma 2})\, s_{\gamma n} I_p(\theta_{\gamma 1}) + 0.2556 \cdot 10^{10} I_{-p+1}(\theta_{\gamma 2}) I_p(\theta_{\gamma 1}) -\\
& 4.4775 s_{\gamma n} I_{-p}(\theta_{\gamma 2}) I_{p+1}(\theta_{\gamma 1}) - 0.2514 \cdot 10^{11} I_{-p}(\theta_{\gamma 2}) I_p(\theta_{\gamma 1}) +\\
& 0.2039 \cdot 10^{12} I_{-p}(\theta_{\gamma 2}) I_p(\theta_{\gamma 1}) \lambda_{\gamma n} - 5.4365 s_{\gamma n} I_{-p}(\theta_{\gamma 2}) I_p(\theta_{\gamma 1}) +\\
& 0.5596 \cdot 10^{10} I_p(\theta_{\gamma 2}) I_{-p+1}(\theta_{\gamma 1}) - 0.5596 \cdot 10^{10} I_{-p}(\theta_{\gamma 2}) I_{p+1}(\theta_{\gamma 1}))\\
=\; & 0
\end{aligned}$$

The task is to find the values of $\lambda_{\gamma n}$ that make $B.C. = 0$. As previously mentioned, the value of $B.C.$ is not real valued, but is complex valued. Therefore in order to find where $B.C. = 0$, we use the fact that its magnitude, $|B.C.|$ should be zero when $B.C. = 0$. In

other words, when:

$$B.C. = \alpha + i\beta \tag{4.68}$$

with magnitude:

$$|B.C.| = \sqrt{\alpha^2 + \beta^2} \tag{4.69}$$

and if:

$$B.C = 0 \tag{4.70}$$

then:

$$|B.C| = 0 \tag{4.71}$$

One may then use conventional root solvers such as *fsolve* in Maple© to find the values of $\lambda_{\gamma n}$ such that $B.C = 0$. The first five values of $\lambda_{\gamma n}$ were found using *fsolve* in Maple© and are listed in Table 4.2. Figure 4.5 depicts the values of the function $|B.C|$ around the first eigenvalue. Although the values of $|B.C|$ appear to be very large (10^9), it was verified that the values of $\lambda_{\gamma n}$ do in fact satisfy $|B.C| = 0$ and when substituted into the general solution given by Equation (4.62), their partial sum does satisfy the ODE in γ_1 (i.e., Equation (4.46).

Table 4.2: First Five Eigenvalues of Linearized Spatial ODE

$\lambda_{\gamma 1} =$	.10666666
$\lambda_{\gamma 2} =$	.35581402
$\lambda_{\gamma 3} =$	.85265051
$\lambda_{\gamma 4} =$	1.6759089
$\lambda_{\gamma 5} =$	2.8276587

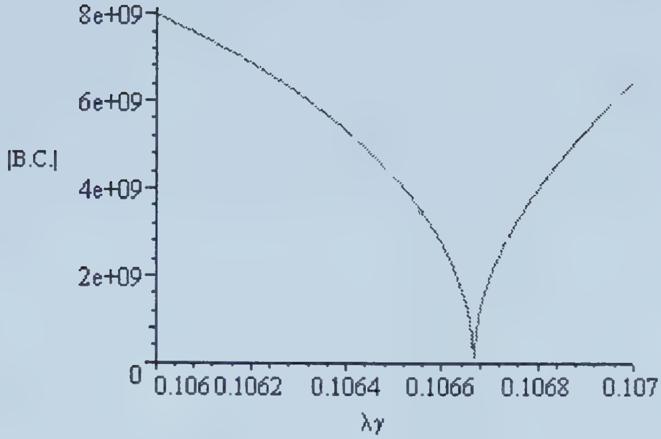

Figure 4.5: First Value of lambda Satisfying $|B.C.|$=0

4.4 Simulation Results

Having found the first five eigenvalues, one can now express the full solution of $\eta_2(z,t)$ using the eigenfunctions and the expression given by Equation (4.45). The procedure is the same as that followed in Chapter 3. Equation (4.72) shows in the first term, the *"unforced"* part of the solution; and the second term represents the *"forced"* part of the solution.

$$\eta_2(z,t) = \sum_{n=0}^{\infty}\left[e^{\lambda_{\gamma n}t}\left\langle \eta_{2,0}, \widetilde{\gamma_{1n}}\right\rangle \gamma_{1n} + \int_0^t e^{\lambda_{\gamma n}(t-s)}\left\langle \eta_1(z,t), \widetilde{\gamma_{1n}}\right\rangle \gamma_{1n} ds\right] \tag{4.72}$$

However in this case, one must note that although we consider only the unforced solution of $\eta_2(z,t)$, (i.e. $\eta_{2,in}(t) = 0$), there is still a *"forced"* part which contains the input term in $\eta_1(z,t)$ given by Equation (4.42). Once again, the parameters used in the simulation are:

- At $t = 0$, initial conditions were such that the reactor had a profile that was slightly greater than that of steady state ($\eta_2(z,0) = 0.01.$).
- It was assumed that there was no deviation from the steady-state value of the input term ($\eta_{2in}(t) = 0$).

Physically, this corresponds to a situation in which the reactor is at a state with a chlorine dioxide (which corresponds to $\eta_2(z,t)$) profile in the reactor that is 0.01 g/l higher than the steady state profile given by Equation (3.20). The solution consists therefore of the evolution of chlorine dioxide concentration in the reactor in time and space from its deviational state of ($\widetilde{C} = 0.01$) down to C_{ss}.(i.e., $\widetilde{C} = 0$).

Figure 4.6 shows the solution using modal decomposition with five modes ($n = 5$). For comparison purposes a finite difference solution with two hundred spatial discretization

points was done (using code from [Renou, 2000]). The finite difference results are shown in Figure 4.7. One may observe that the finite difference solution begins at the desired value of $\widetilde{C} = 0.01$ and progresses smoothly down to $\widetilde{C} = 0$. The modal solution, however has a few oscillations across the reactor at small times ($t < 5$). A comparison was made by integrating the difference between the two solutions in space and in time. The results are shown in Figure 4.8. In general the error is fairly small (i.e., of the order of 10^{-4}). This

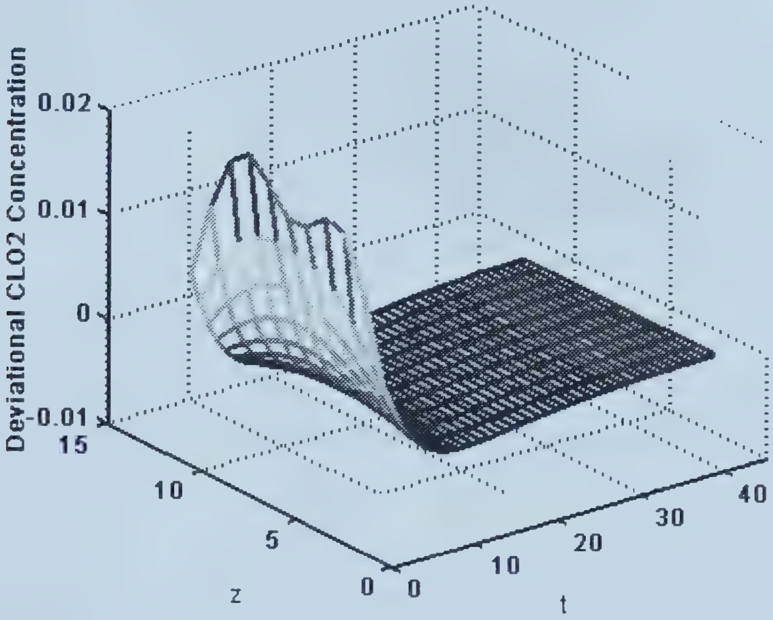

Figure 4.6: Modal Solution of Deviational $\eta_2(z,t)$ (i.e.:$\widetilde{C}(z,t)$) with $n = 5$.

procedure was repeated using $n = 2, 3, 4$ and the difference between the modal method and the finite difference method was calculated in each case. Additional Figures may be seen in Appendix C. In order to see the magnitude of the difference between the two methods, the (using a double integration) was calculated and is plotted in Figure 4.9.

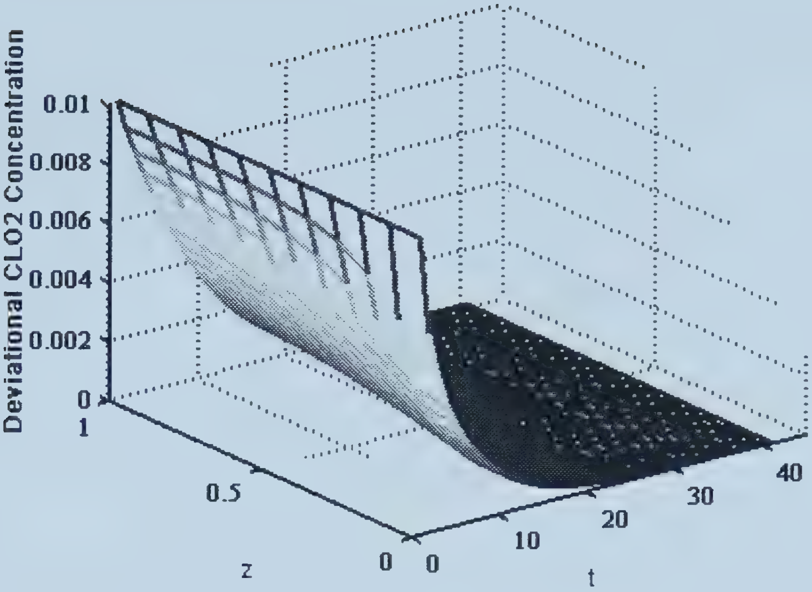

Figure 4.7: Finite Difference Solution of Deviational $\eta_2(z,t)$ (i.e.: $\widetilde{C}(z,t)$) with a Mesh of 200 Points.

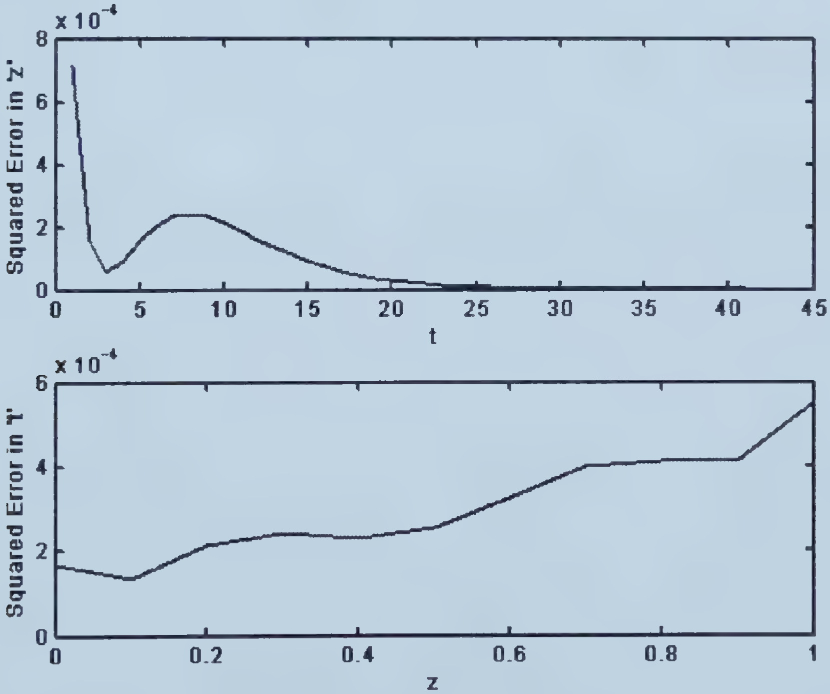

Figure 4.8: Integral of the Difference Between Finite Difference Method and Modal Method ($n = 5$) Over the Space Variable $'z'$ and the Time Variable $'t'$.

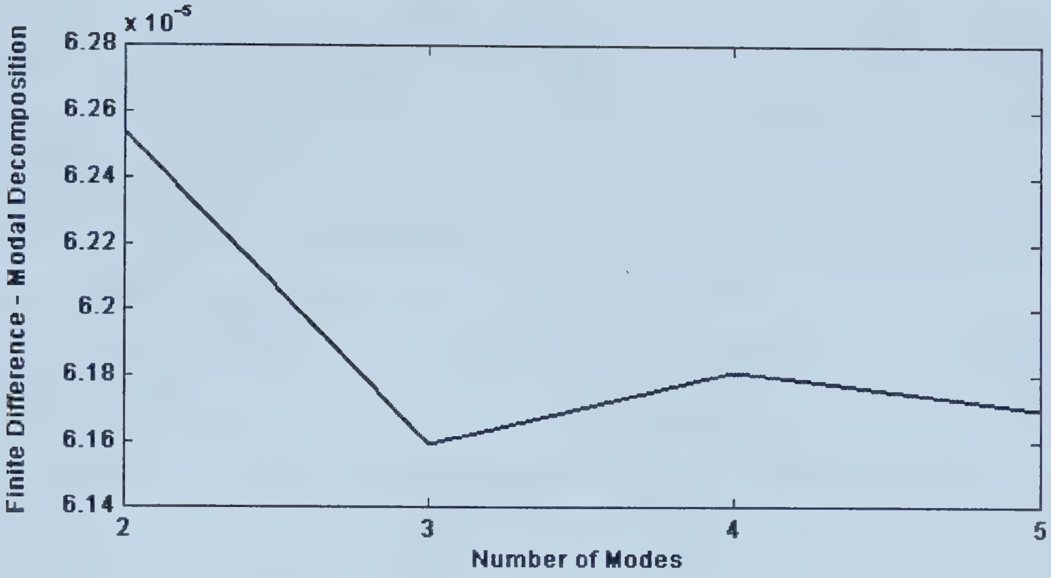

Figure 4.9: Effect of Varying Number of Modes on "Volume" Difference Beween Finite Difference and Modal Methods.

4.4.1 Discussion

Figure 4.9 shows that, in general, the modal approximation converges to the finite difference solution as the modes increase. There is a slight "bump" in the curve at $n = 4$; however, the differences are all within the same order of magnitude, therefore it is difficult to really make any strong conclusions about the jump at four modes, as it could simply be due to the effects of numerical simulation.

It was quite time consuming to find the eigenvalues of $\eta_2(z, t)$ as solving Equation (4.67) was fairly computationally demanding. As a result, only the first five modes were found, and thus we can only draw conclusions on the effect of additional modes up to $n = 5$.

Despite this, the modal decomposition still proves to be a useful tool for simulation and analysis of DPS. [Ray, 1981] shows that modal representation is a very efficient means of simulating a process when there is time-varying control action. Also, in systems where the eigenvalues increase rapidly with increasing n, only a few eigenfunctions are required for representing the system behaviour. Furthermore, a second valuable use of modal decomposition is in the design of control structures [Ray, 1981]. The results of Chapter 3 concur with these findings, as a linear example was used. In the nonlinear example shown in Chapter 4, the results with just five modes were promising and one could conclude that modal decomposition for nonlinear convection-diffusion-reaction systems merits further study. Although the finite difference method is generally a "simpler" method to implement, it contains no spectral information whatsoever. There is therefore much more information in the solution obtained using modal decomposition. Finite difference methods simply partition the system into N parts with each part having a mean value concentration in that part. As the

subdivision becomes finer ($N = 200$ in the case shown above) the size of the state vector increases and the discrete approximation approaches the infinite dimensional continuous representation [Gould, 1969]. This is not the most efficient approach, particularly when one is primarily interested in the slowest modes of the system. This was shown in the results: a modal system of fifth order ($n = 5$) could closely match a solution of two hundredth order ($N = 200$). The modal decomposition with just five modes would therefore have less online computational demand than the finite difference counterpart.

One may suggest that a large amount of analysis was required to get the bleaching reactor model into a "solvable" form for using modal decomposition, and therefore question its practicality compared to other methods. Although the analysis was quite involved, once this procedure was established, the calculations are fairly mechanical thereafter. Also to be noted, is that most of the computation is done off-line, and once the model has been decomposed, the design of a controller in this reduced form would require less online computation time a finite difference counter part. Moreover, the entire procedure in Chapter 4 is applicable to any system that may be described by a convection-diffusion-reaction system that can be modelled by a parabolic PDE set similar to Equation (4.1) For example, this particular case study dealt with bilinear reaction kinetics, however, higher order reaction kinetics may still take advantage of this modal decomposition because once linearized, all models will take the form of Equation (4.3). It is important to note that the framework for converting a convection-diffusion-reaction system with nonlinear kinetics to a lumped parameter system using modal decomposition was established in this chapter. Also, promising results show that further investigation is needed to evaluate this method for future use in controller design.

Chapter 5

Summary and Conclusions

Convection-diffusion-reaction systems are distributed parameter systems modelled by PDEs. These systems are common in the chemical process industry. This thesis was concerned with the analysis of convection-diffusion-reaction models using modal decomposition.

There two major contributions that stemmed from this research. The first contribution was the combination of modal decomposition with Model Predictive Control. This method showed that one could reduce the infinite dimensional system studied to a lumped parameter system with just five modes, and a Model Predictive Controller was then designed in the new lumped modal space. In the linear case studied, it was shown that modal decomposition was an effective solution technique, and only a few modes were necessary to capture the dynamics of the solution. The results were promising for use in the control of distributed parameter systems.

Since many convection-diffusion-reaction systems are nonlinear by their reaction terms, a preliminary investigation was done with the analysis of a nonlinear set of PDEs (describing a industrial pulp bleaching reactor) using modal decomposition. This formed the basis of the second contribution of the research: the development of a procedure for producing a linear tangent model and applying modal decomposition to a nonlinear convection-diffusion-reaction model of a pulp bleaching reactor.

Chapter 2 provided an overview of PDEs, their classification and some common solution techniques. This is important as solution techniques are closely related to the type of PDE. Modal decomposition was introduced using the heat equation, a linear PDE. Chapter 3 expanded on modal decomposition, more specifically to convection-diffusion-reaction systems. A linear model with single reactant was analysed. A practical application of the modal decomposition method was then investigated with the design of a Model Predictive Controller in the modal space. It was seen that five modes were sufficient to approximate the solution. Chapter 4 investigated the use of modal decomposition for nonlinear systems by applying the method to a model of a pulp bleaching reactor modeled by a coupled set of nonlinear PDEs. The model was first linearized around an operating trajectory, as modal decomposition only applicable to linear PDEs. The steady state trajectories were obtained

by numerical integration and curve fitting, yielding exponential functions. As a result, these exponentials appeared as explicit functions of 'z' in the linearized PDE model, complicating their solution The PDE was first decoupled by performing a change of variable. The result was two PDEs, the first independent, and fairly easy to solve, yielding simple eigenfunctions containing sin and cos functions. The modal decomposition of the second PDE, yielded a spatial ODE that required several variable changes before a solution could be found. The resulting eigenfunctions involved Modified Bessel functions of complex order. Comparison with a finite difference scheme with 200 discretization points showed that with only five modes, the difference between the two solutions was small.

Potential future work could involve testing other types of controllers in the modal space (for the linear case), and comparing their performance with the performance of the same controller designed based on some benchmark model using a discretization scheme. Also, in the case of nonlinear models, much more work could be done on testing the limitations of the method when the initial conditions are far from the operating trajectory. Other future work could include more analysis relating the number of modes and the accuracy of the solution for both simulation and control. More comparison could be done on linear versus nonlinear PDEs, as well as comparison of the computational requirements for modal decomposition compared to other lumping techniques (discretization, collocation,...).

Also to be studied in further detail (in the bleaching reactor example) is the relationship between the eigenvalues obtained and the Peclet number. Although only one operating point was shown in Chapter 4, another simulation was done with a larger Peclet number. In Chapter 4, $Pe = 2$, however in a prior simulation where $Pe = 33$, it was found that the eigenvalues were much closer together (and thus would require many more modes to capture the dynamics of the system). Unfortunately, at higher Peclet numbers, the analytical solution of the spatial ODE diverges (see Renou, 2000), and therefore the full solution using modal decomposition could not be shown.

Some preliminary conclusions can be drawn on the relationship between the Peclet number and the eigenvalues. As the Peclet number increases, convection phenomena dominate over diffusion phenomena. In the limit, when diffusion phenomena are small or negligible, the parabolic convection-diffusion-reaction model tends to a hyperbolic model. In this case, modal decomposition is no longer an efficient solution method, as many modes are required to capture the dynamics of the system (the modes of hyperbolic systems have equal 'energy' and thus many are needed to represent the true system dynamics). Therefore we can conclude that this method is applicable to systems only where diffusion phenomena are important (low Peclet numbers).

It is important to restate that although a large amount of analysis was required to get the bleaching reactor model into a "solvable" form for modal decomposition, the mechanics of the procedure was established in this thesis, and it paved the way for future simulations and analysis. In general, one can conclude that in the linear case, the convection-reaction-

diffusion system could be well represented with only a few modes. As a result, this method could valuable for use in control applications, as was shown in Chapter 3, with the design of a Model Predictive Controller in the modal space. For the nonlinear case shown in Chapter 4, it can be concluded that although the method is designed for linear systems, the extension to a nonlinear (modal decomposition of the tangent model) provided a good representation of the solution with a few modes when compared to a simplistic finite difference solution. Chapter 4 developed a framework for converting a convection-diffusion-reaction system with nonlinear kinetics to a lumped parameter system using modal decomposition. Promising results show that further investigation is needed to evaluate this method for future use in controller design. Although the computation of the eigenvalues and eigenfunctions was fairly demanding, the majority of the computation time was off-line computation, and therefore the lumped model could be used in control applications.

Bibliography

Ames, W. F. (1977). *Numerical Methods for Partial Differential Equations.* Academic Press Inc.. New York.

Aris, Rutherford (1999). *Mathematical Modeling A Chemical Engineer's Perspective..* Academic Press. San Diego.

Bastin, G. and D. Dochain (1990). *On-Line Estimation and Adaptive Control of Bioreactors.* Elsevier. Amsterdam.

Bewley, T.R. (2001). Flow control: New challenges for a new renaissance. *Progress in Aerospace Sciences* **37**, 21–58.

Bewley, T.R. and S. Liu (1998). Optimal and robust control and estimation of linear paths to transition.. *Journal of Fluid Mechanics* **365**, 305–349.

Christofides, P.D. (1998). Robust control of parabolic PDE systems. *Chemical Engineering Science* **53**(16), 2949–2965.

Christofides, P.D. and P. Daoutidis (1996*a*). Feedback control of hyperbolic PDE systems. *AICHE Journal* **42**(11), 3063–3086.

Christofides, P.D. and P. Daoutidis (1996*b*). Nonlinear control of diffusion-convection-reaction processes. *Computers in Chemical Engineering* **20**, 1071–1076.

Cohen, D. and A. Poore (1974). Tubular chemical reactors: The lumping approximation and bifurcation of oscillatory states.. *SIAM Journal of Applied Mathematics.* **27**, 416–429.

Cutler, C. R. and B. L. Ramaker (1979). Dynamix matrix control - a computer control algorithm.. In: *AICHE National Meeting.* Houston.

Dence, C. W. and D.W. Reeve (1996). *Pulp Bleaching - Principles and Practice.* TAPPI Press. Atlanta, GA.

Dochain, D. (1994). Contribution to the Analysis and Control of Distributed Parameter Systems with Application to (Bio)Chemical Processes and Robotics.. PhD thesis. Universite Catholique de Louvain. Belgium.

Elisante, E., M. Yoshida and S. Matsumoto (1999*a*). IMC based robust pole placement procedure for Modal control of one-dimensional heat conduction process. *Journal of Chemical Engineering of Japan* **32**(6), 796–802.

Elisante, E., Yoshida M. and S. Matsumoto (1999*b*). IMC based robust pole placement procedure for modal control of one-dimensional heat conduction process.. *Journal of Chemical Engineering of Japan* **32**(6), 796–802.

Gavalas, G. (1968). *Nonlinear Differential Equations of Chemically Reacting Systems.* Springer Verlag. Berlin.

Gay, D. H. and W. H. Ray (1995). Identification and control of distributed parameter systems by means of the singular value decomposition. *Chemical Engineering Science* **50**(10), 1519–1539.

Georgakis, C., R. Aris and N. R. Amundson (1977). Studies in the control of tubular reactors -. *Chemical Engineering Science* **32**, 1359–1369.

Gladwell, I. and R. Wait (1979). *A Survey of Numerical Methods for Partial Differential Equations.* Oxford University Press. Oxford.

Gould, L. A. (1969). *Chemical Process Control: Theory and Applications.* Addison-Wesley Publishing Company. Reading.

Gray, A., G.B. Mathews. Second Edition Prepared by A. Gray and T.M. MacRobert (1931). *A Treatise on Bessel Functions and Their Applications to Physics.* second ed.. MacMillan and Co. Ltd. London.

Hanczyc, E. M. and A. Palazoglu (1992). Eigenvalue inclusion for model approximations to distributed parameter systems. *Industrial and Engineering Chemistry Research* **31**(11), 2538–2546.

Hanczyc, E.M. and A. Palazoglu (1995). Nonlinear control of a distributed parameter process: The case of multiple characteristics.. *Industrial and Engineering Chemistry Research* **34**, 4406–4412.

Lefevre L., Dochain D., Feyo de Azevedo S. and Magnus A. (2000). Analysis of the orthogonal collocation method when applied to the numerical integration of chemical reactor models.. *Computers and Chemical Engineering* **24**(12), 2571–2588.

Mäder, H.F. (1976). *Regelungstechnik* **24**, 347.

Matsumoto, S. and M. Yoshida (1989). A method of design for a controller for a parabolic-type distributed-parameter system. application to one-dimensional thermal conduction.. *International Chemical Engineering* **29**(1), 158–165.

McOwen, R. (1996). *Partial Differential Equations: Methods and Applications.* Prentice-Hall.

Michelsen, M.L. and J. Villadsen (1972). A convenient computational procedure for collocation constants.. *The Chemical Engineering Journal* **4**, 64–68.

Mukadi, Samy (2000). CHE 674 lecture notes: Numerical solutions of engineering problems.

Murphy, G. M. (1960). *Ordinary Differential Equations and Their Solutions.* D. Van Nostrand Company. New Jersey.

Murray-Lasso, M. A. (1965). The Modal Analysis and Synthesis of Linear Distributed Systems, Sc.D. Thesis. PhD thesis. M.I.T.. Cambridge, Mass.

Ogunaki and Ray (1994). *Process Dynamics, Modeling, and Control.* Oxford University Press. New York.

Pearson, J. R. A. (1959). A note on the "danckwerts" boundary conditions for continous flow reactors. *Chemical Engineering Science* **10**, 281–284.

Ray, W. H. (1978). Some recent applications of distributed parameter systems theory - a survey. *Automatica* **14**, 281–287.

Ray, W. H. (1981). *Advanced Process Control.* McGraw-Hill Book Company. New York.

Renou, S. (2000). Commande Non-Lineare D'un Systeme Decrit Par Des Equations Paraboliques: Application Au Procede de Blanchiment. PhD thesis. Genie Chimique, Ecole Polytechnique de Montreal, Montreal.

Richalet, J. A., A Rault J.D. Testud and R. Pouliquen (1978). Model predictive heuristic control. *Automatica* **14**, 413.

Sadek, I. S. and M. A. Bokhari (1998). Optimal control of a parabolic distributed parameter system via orthogonal polynomials. *Optimal Control Applications and Methods.* **19**, 205–213.

Savoie, M. and P. Tessier (1997). A mathematical model for chlorine dioxide delignification.. *Tappi Journal* **80**(6), 145–152.

Shang. H., Forbes, F. and M. Guay (2000). Feedback control of hyperbolic PDE systems. ADCHEM. Pisa, Italy.

Sira-Ramirez, H. (1989). Distributed sliding mode control in systems described by quasilinear partial differential equations. *Systems and Control Letters* **13**, 177.

Smets, I. Y., D. Dochain and J.F. Van Impe. (2001*a*). Optimal spatial temperature control of a steady-state exothermic plug flow reactor. part i: Bang-bang control.. Submitted to ECC 2001.

Smets, I. Y., D. Dochain. and J.F. Van Impe. (2001*b*). Optimal spatial temperature control of a steady-state exothermic plug flow reactor. part II: Singular control. Submitted to ECC2001.

Street, R. L. (1973). *The Analysis and Solution of Partial Differential Equations.* Brooks/Cole Publishing Company. Monterey, California.

Varma, A. and R. Aris (1977). Stirred pots and empty tubes.. In: *Chemical Reactor Theory: A Review* (L. Lapidus and N. Amundson, Eds.). Prentice-Hall. Englewood Cliffe, NJ.. pp. 79–154.

Villadsen, J. and M.L. Michelsen (1978). *Solution of Differential Equation Models by Polynomial Appoximation.*. Prentice Hall International Series in the Physical and Chemical Engineering Sciences.. Prentice Hall. Toronto.

Zauderer, E. (1989). *Partial Differential Equations of Applied Mathematics.* John Wiley and Sons. New York.

Appendix A

Nomenclature

$\mathbf{A}, \mathbf{B}$	State space matrices
a, b, c, d	Coefficients
a_r	Temporal modal state (reactor)
a_T	Temporal modal state (heat transfer case)
A_r	Normalizing coefficients
A_T	Normalizing coefficients
A_0, B	Constants in method of characteristics
$B.C.$	Boundary condition function
b_r	Input temporal function (reactor case)
b_T	Input temporal function (heat transfer case)
C	Chlorine Dioxide Concentration (g/l)
$\widetilde{C}$	Deviational chlorine dioxide concentration
c_i	Weight coefficients in MWR
C_1, C_2	Coefficients
C_o	Instantaneous jump parameter (chlorine dioxide)
C_p	Specific heat
C_{ss}	Steady state chlorine dioxide concentration
D_r	Diffusivity (reactor)
e	Error in modal state
f, g	Functions for defining inner products and norms
F	Function
G	Normalizing coefficients
h	Element distance in finite differences
I_p	Modified Bessel function of order p
k_c	Kinetic constant for Chlorine Dioxide
k_l	Kinetic constant for Lignin
K_p	Modified Bessel function of the second kind, order p
k_r	Kinetic constant (1/s)
K_r	Normalizing constant
k_T	Thermal conductivity
l	Length of rod or reactor (m)
L	Lignin Concentration (Kappa)

$\widetilde{L}$	Deviational lignin concentration
L_{in}	Inlet lignin concentration (Kappa)
L_o	Instantaneous jump parameter (lignin)
L_{ss}	Steady state lignin concentration
$L(\cdot)$	Linear operator
n	Number of modes
N	Number of discretization points (F.D.) or functions in MWR
O	Order of error (method of finite difference)
p	Order of Bessel Function
p_h	Prediction horizon
p_ψ	Temporal modal state (of η_1)
q	Temporal modal state of input (of η_1)
$Q(z,t)$	Heat flux distribution
R_e	Residual in MWR
r	Temporal modal state (of η_2)
$s^2_{\psi n}$	Function related to eigenvalues
s_r	Function associated with eigenvalues (reactor case)
$s_{\gamma n}$	Function associated with eigenvalues (nonlinear case)
t	Time (s)
$\widehat{t}$	Dimensionless time
T	Temperature (C)
T_0	Initial temperature distribution
u	Input/manipulated variable
v	Superficial fluid velocity (m/s)
w_i	Weight coefficients in MWR
x	State variable
x_r	Reactant concentration
$x_{r,in}$	Inlet reactant concentration
$x_{r,0}$	Initial reactant concentration
y	Space variable (2-D) (m)
z	Space coordinate (m)
$\widehat{z}$	Dimensionless space coordinate

Greek Letters

α, β	Constants in complex number
β_1, β_2	Transformed variables in the numerical solution of C_{ss} and L_{ss}
β_i	Basis functions in MWR
γ_1	Eigenfunctions (of η_2)
$\widetilde{\gamma_{1n}}$	Eigenfunctions of adjoint operator (of η_2)
δ	Delta distribution
η_1	Combined deviational reactant concentration
η_2	Deviational chlorine dioxide concentration
$\theta_{\gamma 2}, \theta_{\gamma 2}, .$	Constants in $B.C$
λ_r	Eigenvalues (reactor case)
λ_T	Eigenvalues (heat transfer case)
λ_γ	Eigenvalues of (of η_2)
λ_ψ	Eigenvalues (of η_1)
$\mu(z)$	Sturm-Liouville function
ξ_1	Combined steady state reactant concentration ($k_c L_{ss} - k_l C_{ss}$)
ξ_2	Steady state chlorine dioxide concentration C_{ss}
ρ_d	Density
$\rho(z)$	Sturm-Liouville function
ϕ_r	Eigenfunctions (reactor)
ϕ_T	Eigenfunction (heat transfer case)
ψ	Eigenfunctions of η_1
$\widetilde{\psi}$	Eigenfunctions of the adjoint operator to ψ
$\varpi, \gamma_2, \zeta, a, b, c, d, f$	Variables used for state transformations
Ψ	Thermal diffusivity
Ω	Domain in MWR

Appendix B

PDE Solution Methods

Chapter 2 briefly outlined a number of PDE solution methods, this appendix provides further details on this topic.

B.1 Method of Characteristics

The method of characteristics is most commonly used to solve hyperbolic PDEs. For example, using the first order hyperbolic PDE:

$$\frac{\partial x(z,t)}{\partial t}+v\frac{\partial x(z,t)}{\partial z}=A_0x(z,t)+Bu(z,t) \tag{B.1}$$

$$x(0,t)=B_0u_0(t) \tag{B.2}$$

Then defining lines or characteristics

$$\frac{dz}{dt}=v \text{ or } t-\frac{1}{v}z=const. \tag{B.3}$$

One obtains the solution of Equation (B.1) as

$$\left.\frac{dx}{dt}\right|_0=A_0x+Bu \tag{B.4}$$

where the notation $\left.\frac{dx}{dt}\right|_0$ denotes the fact that the solution is taken along a characteristic line defined by Equation (B.3). To obtain the entire solution, one must repeat the solution of Equation (B.4) at different values of t_0 [Ray, 1981].

Ray explains that solving the equations along a characteristic line corresponds to following the changes in an element of material moving from $z = 0$ to $z = l$ with a velocity v.

B.2 Finite Differences

There are two methods for solving PDEs using finite difference approximations. The first method is full discretization of the PDE in both time and space yielding a system of algebraic equations. The second method uses semi-discretization for the spatial derivatives, resulting in a system of ODEs in time. This process is sometimes called the method of lines. One may then use any available software to solve the resulting system of ODEs in time [Mukadi, 2000]. This is the preferred method and the one chosen for any finite difference solutions shown in this thesis.

Stability of the difference schemes must be considered prior to selecting difference approximations. For instance, for full discretization of the standard parabolic heat equation seen in Equation (1.1), the spatial discretization should be approximated using a second order central difference for the spatial discretization and a forward difference approximation for the temporal discretization. Although this leads to a larger truncation error, it can be shown in [Street, 1973] that using the central difference scheme for the temporal discretization leads to a solution that is always unstable. In the cases where the method of lines is used, one may check stability by making sure the selection of the difference schemes result in stable (left plane) eigenvalues of the A matrix.

$$\frac{\partial x(z,t)}{\partial t} \approx Ax + b \tag{B.5}$$

where the vector x for N discretization points is

$$x = [x_1, x_2, x_3, ...x_N]^T \tag{B.6}$$

The following table lists the most common difference schemes shown here for spatial discretization.

Table B.1: Finite Difference Approximations

First order forward difference	$\frac{\partial x(z,t)}{\partial z} \approx \frac{x(z+h,t)-x(z,t)}{h}$	Error $= O(h)$
First order backward difference	$\frac{\partial x(z,t)}{\partial z} \approx \frac{x(z,t)-x(z-h,t)}{h}$	Error $= O(h)$
First order central difference	$\frac{\partial x(z,t)}{\partial z} \approx \frac{x(z+h,t)-x(z-h,t)}{2h}$	Error $= O(h^2)$
Second order central difference	$\frac{\partial^2 x(z,t)}{\partial z^2} \approx \frac{x(z+h,t)-2x(z,t)+x(z-h,t)}{h}$	Error $= O(h^2)$

Appendix C

Model Predictive Control Results

Model predictive control was applied in the modal space in Chapter 3. The following two sections are dedicated to mathematical definitions used in the computations and simulations results, respectively.

C.1 Preliminary Definitions

The second order differential operator defined over $0 < z < 1$:

$$L(\cdot) = a(z)\frac{d^2(\cdot)}{dz^2} + b(z)\frac{d(\cdot)}{dz} + c(z)(\cdot) \tag{C.1}$$

has an adjoint operator $L^*(\cdot)$ defined [Ray, 1981] so that for any two functions $x_1(z), x_2(z)$:

$$\int_0^1 x_1(z)L(x_2(z))dz = \int_0^1 x_2(z)L^*(x_1(z))dz \tag{C.2}$$

where the adjoint operator is defined as:

$$L^*(\cdot) = a(z)\frac{d^2(\cdot)}{dz^2} - b(z)\frac{d(\cdot)}{dz} + c(z)(\cdot) \tag{C.3}$$

An operator which is identical to its adjoint is termed *self-adjoint*. Self-adjoint operators have some distinct properties: together with homogenous boundary conditions, a self-adjoint differential operator produces orthogonal eigenfunctions. If the operator happens to be non-self-adjoint, it is generally possible to invoke a change of variable or if the operator is of the form:

$$L(\cdot) = \frac{1}{\rho(z)}\frac{d}{dz}\left[\mu(z)\frac{d(\cdot)}{dz}\right] + c(z)(\cdot) \tag{C.4a}$$

it is possible to use Sturm Liouville theory [Ray, 1981], which states that the system:

$$Lx = \lambda x \tag{C.5}$$

coupled with homogeneous boundary conditions will have a discrete spectrum of eigenvalues λ_n and a corresponding set of eigenfunctions $\phi_n(z)$ which are orthogonal with respect to

$\rho(z)$, i.e.[Ray, 1981]:

$$\int_0^1 \rho(z)\phi_n(z)\phi_m(z)dz = 0 \qquad n \neq m \tag{C.6}$$

The definitions detailed above are used in the modal decomposition procedure. The definitions and properties of self-adjoint operators are used in the modal decomposition of the reactor example in Chapter 3, as the spatial ODE is non self-adjoint, and one must use the definitions in Equations (C.2)-(C.6) to solve the ODE.

C.2 Simulations

Simulations of the linear convection-reaction-diffusion system were done in Chapter 3. A Model Predictive Controller was applied to the system, and the simulations were run, varying the number of modes. Below are the setpoint and steady state profiles of the results from Chapter 3, using five and ten modes.

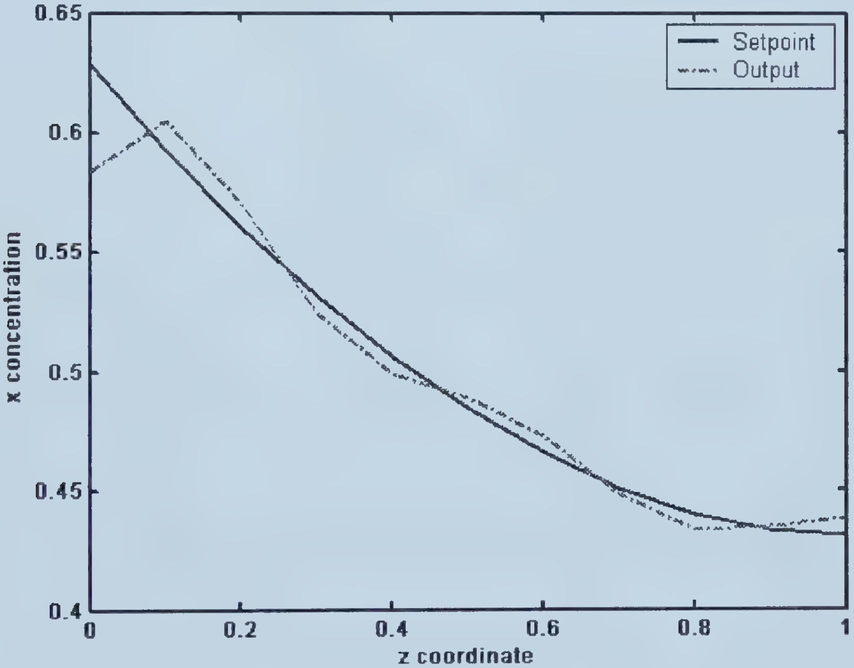

Figure C.1: Setpoint and Actual Output Concentration at Steady State ($t = 55$) using MPC ($n = 5$) at .

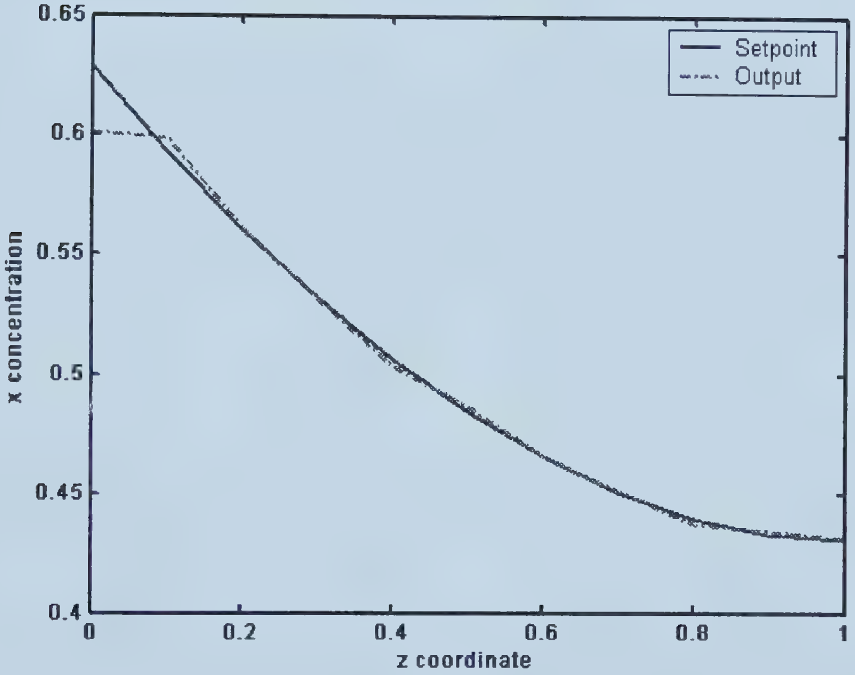

Figure C.2: Setpoint and Actual Output Concentration at Steady State ($t = 55$) using MPC ($n = 10$).

Appendix D

Bessel and Modified Bessel Functions

The solution to Bessel's equation, (given by Equation (4.60)) are two linearly independent solutions called Bessel functions of the p^{th} order. They are obtained by a power series expansion and the Method of Frobenius which is detailed in [Street, 1973]. The recursion relations for common Bessel functions of the first and second kind ($J_p(z)$ and $Y_p(z)$) are found in the table below. Typical plots of Bessel Functions of the first and second kind are shown in Figure D.1, and their values are tabulated in mathematical handbooks for several integer and some non integer orders.

Table D.1: Bessel Functions of the First and Second Kind

$J_0(z) =$	$\sum\limits_{m=0}^{\infty} (-1)^m \frac{z^{2m}}{2^{2m}(m!)^2}$	$p = 0$
$J_p(z) =$	$\sum\limits_{m=0}^{\infty} (-1)^m \frac{z^{P+2m}}{2^{P+2m} m!(p+m)!}$	p a non zero integer
$Y_p(z) =$	$\frac{2}{\pi} \ln \frac{z}{2} J_p(z) + O(z^{-P}) + O(z^P)$	p a non zero integer
$J_p(z) =$	$\sum\limits_{m=0}^{\infty} \frac{(-1)^m z^{P+2m}}{2^{-P+2m} m!\Gamma(m-p+1)!}$	p neither an integer or zero
$J_{-p}(z) =$	$\sum\limits_{m=0}^{\infty} \frac{(-1)^m z^{-P+2m}}{2^{-P+2m} m!\Gamma(m-p+1)!}$	p neither an integer or zero

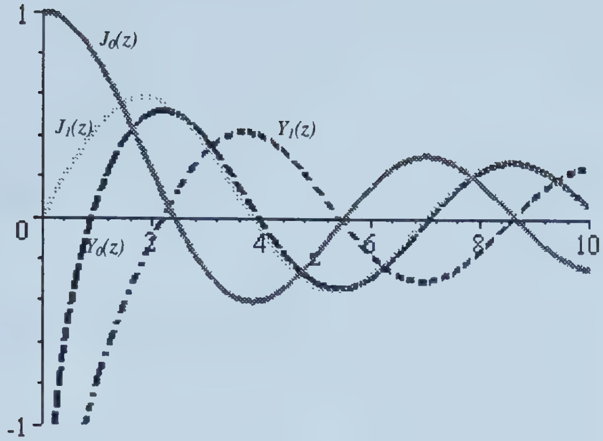

Figure D.1: Bessel Functions of the First and Second Kind of Orders 0 and 1.

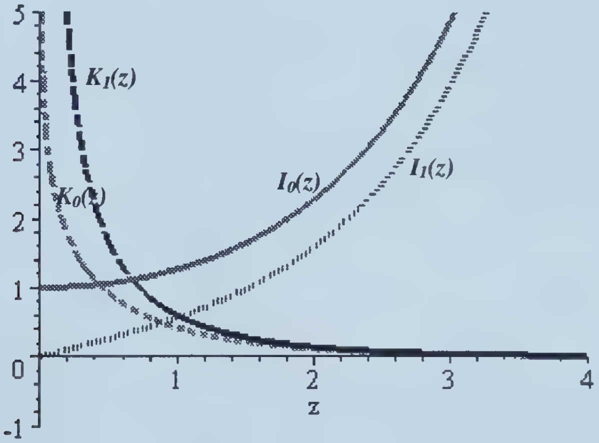

Figure D.2: Modified Bessel Functions of Integer Orders.

If the argument (ϖ_5 is the argument in Equation (4.60)) is non-real, then one must use the transformation $\varpi_5 = i\varpi_6$, where $i = \sqrt{-1}$. Bessel's ODE then becomes Bessel's Modified Equation (as in Equation (4.60)), and the solutions are two linearly independent solutions called Bessel's Modified functions of the first and second kind. There are defined as follows:

$$\begin{aligned} I_p &= i^{-p} J_p(iz) \\ K_p &= \frac{\pi}{2} i^{n+1} \left[J_p(iz) + iY_p(iz) \right] \end{aligned} \tag{D.1}$$

Typical plots of modified Bessel functions of order zero are shown in Figure D.2. Note that they differ greatly from the plots of Bessel functions in that they are neither periodic, nor bounded.

Appendix E

Modal Simulations

Below are additional figures from those shown in Chapter 4, representing the simulations done on the pulp bleaching reactor model.

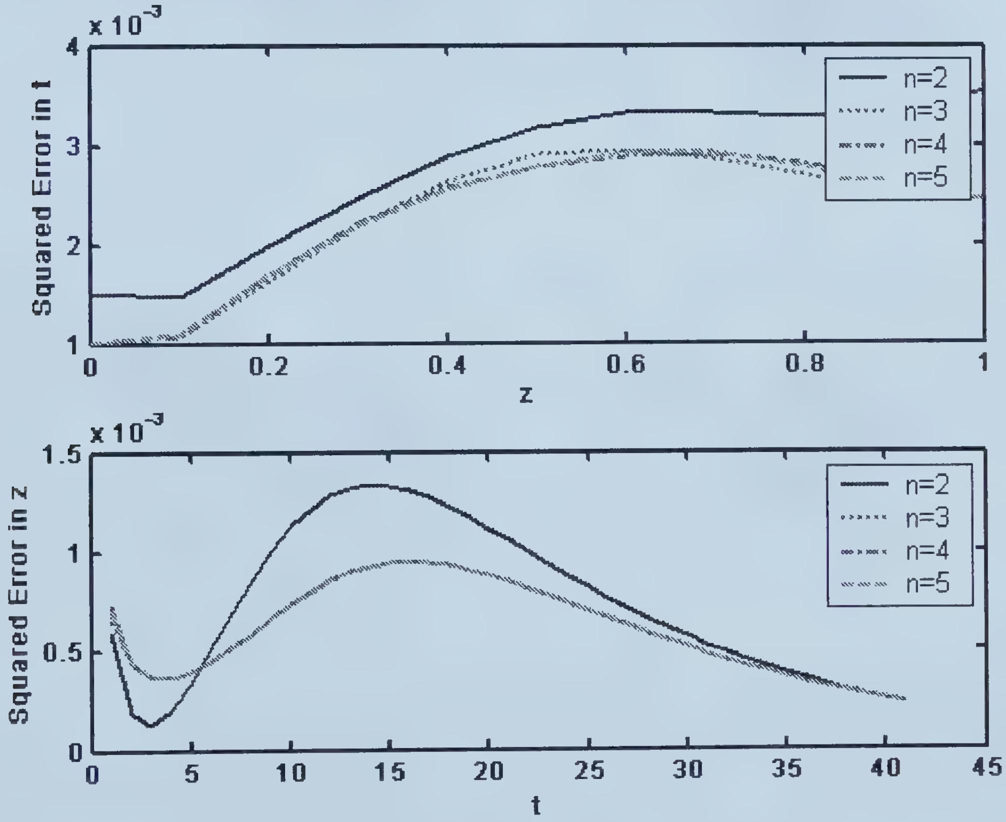

Figure E.1: Integral of the Difference Between Modal and Finite Difference Solutions for $n = 2, 3, 4$ and 5.

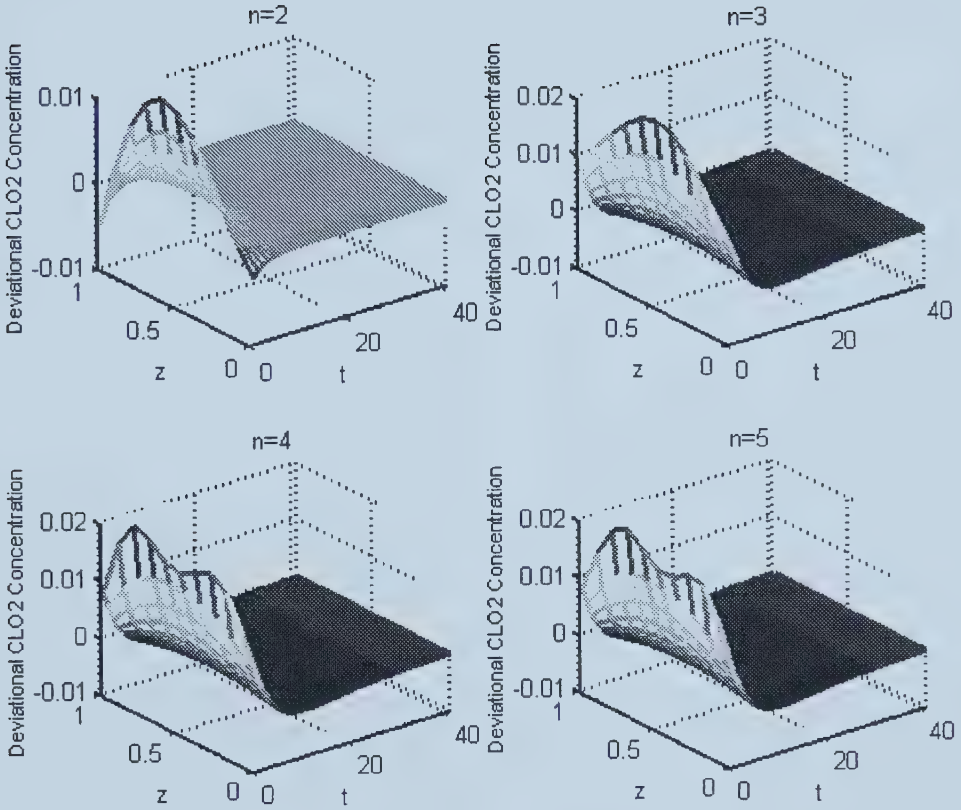

Figure E.2: Deviational Chlorine Dioxide Concentration Profiles Using Modal Deomposition for $n = 2, 3, 4, 5$.

University of Alberta Library
0 1620 1492 0175

B45430